

SUPPLEMENTARY INFORMATION

Synthesis and anticancer activity of carbosilane metallodendrimers based on arene ruthenium (II) complexes.

**Marta Maroto-Díaz ^{ac}, Benelita T. Elie ^{d,e}, Pilar Gómez-Sal ^a, Jorge Pérez-Serrano ^b,
Rafael Gómez ^{*ac}, Maria Contel ^{*d,e}, F. Javier de la Mata ^{*ac}**

^aDepartamento de Química Orgánica y Química Inorgánica, Universidad de Alcalá, Campus Universitario, E-28871 Alcalá de Henares, Spain. E-mail: javier.delamata@uah.es. Fax: +34 91 885 4683

^bDepartamento de Biomedicina y Biotecnología, Universidad de Alcalá, Campus Universitario, E-28871 Alcalá de Henares, Spain.

^cNetworking Research Center on Bioengineering, Biomaterials and Nanomedicine (CIBER-BBN), Spain.

^dDepartment of Chemistry, Brooklyn College and The Graduate Center, The City University of New York, Brooklyn, New York 11210, United States. E-mail: mariacontel@brooklyn.cuny.edu

^eBiology PhD Program, The Graduate Center, The City University of New York, 365 Fifth Avenue, New York, NY, 10016, United States.

Table of Contents

1. Synthesis of dendritic ligands **3, 6** and **9**
2. Synthesis of carbosilane metallodendrimers based on arene ruthenium (II) complexes **13-15** and **19-21**
3. **Figure S1-S9.** Selected ^1H -NMR and ^{13}C -NMR spectra of dendritic ligands (**1-9**)
4. **Figure S10-S17.** Selected ^1H -NMR and ^{13}C -NMR spectra of carbosilane metallodendrimers based on arene ruthenium (II) complexes (**10, 11, 13-15, 17,18**)
5. **Scheme S1. Figure S18-S19.** ^1H and ESI-TOF mass spectra of the reaction S1
6. **Scheme S2. Figure S20-S21.** ^1H and ^{13}C -NMR spectra of the reaction S2
7. **Scheme S3. Figure S22.** ^1H and ^{13}C -NMR spectra of the reaction S3
8. **Figure S23-S35.** Stability tests
9. **Figure S36-S45.** Fluorescence titration curve of HSA with compound **10-11, 13-15** and **17-18**
10. **Table S1-S2.** Crystal and structure refinement data for compound **10**

1. Synthesis of dendritic ligands **3**, **6** and **9** and NMR spectra data

Second generation dendrimers. G₂-[NCPh(*p*-N)]₈ (**3**), G₂-[NCPh(*o*-N)]₈ (**6**) and G₂-[NCPh(*o*-OH)]₈ (**9**).

To a solution of G₂-[NH₂]₈ (240 mg, 0.14 mmol) in THF, the corresponding aldehyde, 4-pyridinecarboxaldehyde (127.3 mg, 1.19 mmol) for (**3**), 2-pyridinecarboxaldehyde (127.3 mg, 1.19 mmol) for (**6**), and salicylaldehyde (145.1 mg, 1.19 mmol) for (**9**) was added. The mixture was stirred under inert atmosphere at room temperature in the presence of anhydrous MgSO₄ for 24 hour. Afterwards, the solvent was rotary evaporated to give an oil that was purified by size exclusion chromatography.

G₂-[NCPh(*p*-N)]₈ (**3**). Yellow pale oil, yield 250 mg (72%). ¹H-NMR (CDCl₃): δ (ppm) = -0.13 (s, 12H, -CH₃SiCH₂CH₂CH₂Si); -0.07 (s, 48H, -(CH₃)₂SiCH₂CH₂CH₂N); 0.48 (overlapping br m, 64H, -SiCH₂CH₂CH₂Si, -CH₃SiCH₂CH₂CH₂Si and -(CH₃)₂SiCH₂CH₂CH₂N); 1.25 (overlapping br m, 24H, -SiCH₂CH₂CH₂Si and -CH₃SiCH₂CH₂CH₂Si), 1.65 (br m, 16H, -(CH₃)₂SiCH₂CH₂CH₂N); 3.59 (t, ³J (*H-H*) = 6.8 Hz, 16H, -(CH₃)₂SiCH₂CH₂CH₂N); 7.54 (m, 16H, Ar); 8.63 (m, 16H, Ar); 8.20 (s, 8H, -CH_{imine}). ¹³C{¹H}-NMR (CDCl₃): δ (ppm) = -4.8 (-(CH₃)₂SiCH₂CH₂CH₂N); -3.2 (-CH₃SiCH₂CH₂CH₂Si); 13.2 (-(CH₃)₂SiCH₂CH₂CH₂N); 18.6, 18.7, 18.9, 20.1 (-SiCH₂CH₂CH₂Si and -CH₃SiCH₂CH₂CH₂Si); 25.4 (-(CH₃)₂SiCH₂CH₂CH₂N); 65.4 (-(CH₃)₂SiCH₂CH₂CH₂N); 122.0, 143.1, 150.5 (C_{Ar}); 158.9 (-CH_{imine}). ²⁹Si-NMR (CDCl₃): δ (ppm) = -SiCH₂CH₂CH₂Si is not observed; 0.85 (-CH₃SiCH₂CH₂CH₂Si); 1.88 (-(CH₃)₂SiCH₂CH₂CH₂N). ¹⁵N NMR (CDCl₃): δ (ppm) = -64.5 (N_{pyr}); -32.2

($\mathbf{N}_{\text{imine}}$). Elemental Analysis (%): Calc. For $\text{C}_{128}\text{H}_{220}\text{N}_{16}\text{Si}_{13}$ (2348.34): C, 65.27; H, 9.44; N, 9.54; Found: C, 64.98; H, 9.33; N, 9.26.

$\text{G}_2\text{-[NCP}(\textit{o}\text{-N})\text{]}_8$ (**6**). Brown oil, yield 273 mg (79%). $^1\text{H-NMR}$ (CDCl_3): δ (ppm) = -0.11 (s, 12H, $-\text{CH}_3\text{SiCH}_2\text{CH}_2\text{CH}_2\text{Si}$); -0.05 (s, 48H, $-(\text{CH}_3)_2\text{SiCH}_2\text{CH}_2\text{CH}_2\text{N}$); 0.53 (overlapping br m, 64H, $-\text{SiCH}_2\text{CH}_2\text{CH}_2\text{Si}$, $-\text{CH}_3\text{SiCH}_2\text{CH}_2\text{CH}_2\text{Si}$ and $-(\text{CH}_3)_2\text{SiCH}_2\text{CH}_2\text{CH}_2\text{N}$); 1.28 (overlapping br m, 24H, $-\text{SiCH}_2\text{CH}_2\text{CH}_2\text{Si}$ and $-\text{CH}_3\text{SiCH}_2\text{CH}_2\text{CH}_2\text{Si}$); 1.69 (br m, 16H, $-(\text{CH}_3)_2\text{SiCH}_2\text{CH}_2\text{CH}_2\text{N}$); 3.63 (t, $^3J_{(\text{H-H})} = 7.0$ Hz, 16H, $-(\text{CH}_3)_2\text{SiCH}_2\text{CH}_2\text{CH}_2\text{N}$); 7.28 (m, 8H, Ar); 7.71 (m, 8H, Ar); 7.97 (m, 8H, Ar); 8.62 (m, 8H, Ar); 8.35 (s, 8H, $-\text{CH}_{\text{imine}}$). $^{13}\text{C}\{^1\text{H}\}\text{-NMR}$ (CDCl_3): δ (ppm) = -4.8 ($-(\text{CH}_3)_2\text{SiCH}_2\text{CH}_2\text{CH}_2\text{N}$); -3.2 ($-\text{CH}_3\text{SiCH}_2\text{CH}_2\text{CH}_2\text{Si}$); 13.2 ($-(\text{CH}_3)_2\text{SiCH}_2\text{CH}_2\text{CH}_2\text{N}$); 18.6, 18.7, 18.9, 20.2 ($-\text{SiCH}_2\text{CH}_2\text{CH}_2\text{Si}_{\text{core}}$ and $-\text{CH}_3\text{SiCH}_2\text{CH}_2\text{CH}_2\text{Si}$); 25.5 ($-(\text{CH}_3)_2\text{SiCH}_2\text{CH}_2\text{CH}_2\text{N}$); 65.1 ($-(\text{CH}_3)_2\text{SiCH}_2\text{CH}_2\text{CH}_2\text{N}$); 121.3, 124.7, 136.6, 149.5, 161.8 (C_{Ar}); 154.8 ($-\text{CH}_{\text{imine}}$). $^{29}\text{Si-NMR}$ (CDCl_3): δ (ppm) = $-\text{SiCH}_2\text{CH}_2\text{CH}_2\text{Si}$ is not observed; 0.90 ($-\text{CH}_3\text{SiCH}_2\text{CH}_2\text{CH}_2\text{Si}$); 1.90 ($-(\text{CH}_3)_2\text{SiCH}_2\text{CH}_2\text{CH}_2\text{N}$). $^{15}\text{N NMR}$ (CDCl_3): δ (ppm) = -67.4 (\mathbf{N}_{pyr}); -38.0 ($\mathbf{N}_{\text{imine}}$). Elemental Analysis (%): Calc. For $\text{C}_{128}\text{H}_{220}\text{N}_{16}\text{Si}_{13}$ (2348.34): C, 65.47; H, 9.44; N, 9.54; Found: C, 65.04; H, 8.96; N, 9.72.

$\text{G}_2\text{-[NCP}(\textit{o}\text{-OH})\text{]}_8$ (**9**). Yellow oil, yield 306 g (84%). $^1\text{H-NMR}$ (CDCl_3): δ (ppm) = -0.09 (s, 12H, $-\text{CH}_3\text{SiCH}_2\text{CH}_2\text{CH}_2\text{Si}$); -0.04 (s, 48H, $-(\text{CH}_3)_2\text{SiCH}_2\text{CH}_2\text{CH}_2\text{N}$); 0.54 (overlapping br m, 64H, $-\text{SiCH}_2\text{CH}_2\text{CH}_2\text{Si}$, $-\text{CH}_3\text{SiCH}_2\text{CH}_2\text{CH}_2\text{Si}$ and $-(\text{CH}_3)_2\text{SiCH}_2\text{CH}_2\text{CH}_2\text{N}$); 1.27 (overlapping br m, 24H, $-\text{SiCH}_2\text{CH}_2\text{CH}_2\text{Si}$ and $-\text{CH}_3\text{SiCH}_2\text{CH}_2\text{CH}_2\text{Si}$); 1.66 (br m, 16H, $-(\text{CH}_3)_2\text{SiCH}_2\text{CH}_2\text{CH}_2\text{N}$); 3.55 (t, $^3J_{(\text{H-H})} = 6.5$ Hz, 16H, $-(\text{CH}_3)_2\text{SiCH}_2\text{CH}_2\text{CH}_2\text{N}$); 6.85 (m, 8H, Ar); 6.94 (m, 8H, Ar); 7.26 (m, 16H, Ar); 8.30 (s, 8H, $-\text{CH}_{\text{imine}}$); $-\text{OH}$ is not observed. $^{13}\text{C}\{^1\text{H}\}\text{-NMR}$ (CDCl_3): δ

(ppm) = -4.8 (-CH₃)₂SiCH₂CH₂CH₂N); -3.2 (-CH₃SiCH₂CH₂CH₂Si); 13.0 (-CH₃)₂SiCH₂CH₂CH₂N); 18.6, 18.7, 18.9, 20.1 (-SiCH₂CH₂CH₂Si and -CH₃SiCH₂CH₂CH₂Si); 25.7 (-(CH₃)₂SiCH₂CH₂CH₂N); 62.9 (-(CH₃)₂SiCH₂CH₂CH₂N); 117.2, 118.5, 118.9, 131.2, 132.2, 164.6 (C_{Ar}); 161.6 (-CH_{imine}). ²⁹Si-NMR (CDCl₃): δ (ppm) = -SiCH₂CH₂CH₂Si is not observed; 0.97 (-CH₃SiCH₂CH₂CH₂Si); 2.00 (-(CH₃)₂SiCH₂CH₂CH₂N). ¹⁵N NMR (CDCl₃): δ (ppm) = -82.9 (N_{imine}). Elemental Analysis (%): Calc. For C₁₃₆H₂₂₈N₈O₈Si₁₃ (2468.43): C, 66.17; H, 9.31; N, 4.54; Found: C, 65.78; H, 9.19; N, 4.95.

2. *Synthesis and characterization of carbosilane metallodendrimers based on arene ruthenium (II) complexes 13-15 and 19-21*

Neutral N- metallodendrimers. G_0 -[NCPh(*p*-N)Ru(η^6 -*p*-cymene)Cl₂]₁ (**13**), G_1 -[NCPh(*p*-N)Ru(η^6 -*p*-cymene)Cl₂]₄ (**14**) and G_2 -[NCPh(*p*-N)Ru(η^6 -*p*-cymene)Cl₂]₈ (**15**).

To a solution of the dendritic ligand (86.5 mg, 0.33 mmol of G_0 -[NCPh(*p*-N)]₁; 95 mg, 0.09 mmol of G_1 -[NCPh(*p*-N)]₄; 96.8 mg, 0.04 mmol of G_2 -[NCPh(*p*-N)]₈) in dichlorometane was slowly added the dimer [Ru(η^6 -*p*-cymene)Cl₂]₂ (101 mg, 0.16 mmol for G_0 -[NCPh(*p*-N)Ru(η^6 -*p*-cymene)]₁ (**13**); 114 mg, 0.19 mmol for G_1 -[NCPh(*p*-N)Ru(η^6 -*p*-cymene)]₄ (**14**) and 101 mg, 0.16 mmol for G_2 -[NCPh(*p*-N)Ru(η^6 -*p*-cymene)]₈ (**15**). The reaction was allowed to stir at room temperature for 5h. The mixture solution was concentrated, and the product, a yellow-orange solid, was precipitated with diethyl ether and dried *in vacuo*.

G_0 -[NCPh(*p*-N)Ru(η^6 -*p*-cymene)Cl₂]₁ (**13**). Yellow-orange solid, yield 102 mg (55%). ¹H-NMR (CDCl₃): δ (ppm) = 0.52 (overlapping m, 8H, -Si(CH₂CH₃)₃ and -SiCH₂CH₂); 0.92 (m, 9H, -Si(CH₂CH₃)₃); 1.30 (d, ³J (*H-H*) = 6.9 Hz, 6H, -(CH₃)₂CH_{cye}); 1.68 (m, 2H, -SiCH₂CH₂CH₂N); 2.09 (s, 3H, -CH_{3cye}); 2.98 (m, 1H, -(CH₃)₂CH_{cye}); 3.66 (t, ³J (*H-H*) = 6.6 Hz, 2H, -SiCH₂CH₂CH₂N); 5.22 (d, ³J (*H-H*) = 6.0 Hz, 2H, Ar_{cye}); 5.44 (d, ³J (*H-H*) = 6.0 Hz, 2H, Ar_{cye}); 7.59 (m, 2H, Ar); 9.08 (m, 2H, Ar); 8.25 (s, 1H, -CH_{imine}). ¹³C {¹H}-NMR (CDCl₃): δ (ppm) = 3.4 (-Si(CH₂CH₃)₃); 7.6 (-Si(CH₂CH₃)₃); 9.1 (-SiCH₂CH₂); 18.4 (-CH_{3cye}); 22.4 (-CH₃)₂CH_{cye}); 25.3 (-SiCH₂CH₂CH₂N); 30.8 (-CH₃)₂CH_{cye}); 65.6 (-SiCH₂CH₂CH₂N); 82.3, 83.2 (-CH_{cye}); 97.4, 103.7 (C_{cye}); 122.6, 144.6, 155.4 (CAr); 157.4 (-CH_{imine}). ²⁹Si-NMR (CDCl₃): δ (ppm) = 7.11 (-Si(CH₂CH₃)₃). Elemental

Analysis (%): Calc. For C₂₅H₄₀Cl₂N₂RuSi (568.66): C, 57.68; H, 7.71; N, 2.49; Found: C, 57.76; H, 7.42; N, 2.57.

G₁-[NCP(*p*-N)Ru(η⁶-*p*-cymene)Cl₂]₄ (**14**). Yellow-orange solid, yield 74.8 mg (55%). ¹H-NMR (CDCl₃): δ (ppm) = -0.04 (br s, 24H, -(CH₃)₂SiCH₂CH₂CH₂N); 0.54 (overlapping m, 24H, -SiCH₂CH₂CH₂Si and -SiCH₂CH₂CH₂N); 1.30 (overlapping br m, 32H, -(CH₃)₂CH_{cye} and -SiCH₂CH₂CH₂Si); 1.66 (br m, 8H, -SiCH₂CH₂CH₂N); 2.07 (s, 12H, -CH_{3cye}); 2.97 (br m, 4H, -(CH₃)₂CH_{cye}); 3.63 (br m, 8H, -SiCH₂CH₂CH₂N); 5.24 (m, 8H, Ar_{cye}); 5.46 (m, 8H, Ar_{cye}); 7.55 (m, 8H, Ar); 9.04 (m, 8H, Ar); 8.20 (s, 4H, -CH_{imine}). ¹³C {¹H}-NMR (CDCl₃): δ (ppm) = -3.1 (-(CH₃)₂SiCH₂CH₂CH₂N); 13.2 (-SiCH₂CH₂CH₂N); 17.5, 18.3, 18.6 (-SiCH₂CH₂CH₂Si); 20.3 (-CH_{3cye}); 22.5 (-(CH₃)₂CH_{cye}); 25.4 (-SiCH₂CH₂CH₂N); 30.3 (-(CH₃)₂CH_{cye}); 65.4 (-SiCH₂CH₂CH₂N); 82.3, 83.3 (-CH_{cye}); 97.4, 103.6 (C_{cye}); 122.7, 144.5, 155.4 (CAr); 157.6 (-CH_{imine}). ²⁹Si-NMR (CDCl₃): δ (ppm) = 0.60 (-SiCH₂CH₂CH₂Si), 2.00 (-(CH₃)₂SiCH₂CH₂CH₂N). Elemental Analysis (%): Calc. For C₉₆H₁₄₈Cl₈N₈Ru₄Si₅ (2242.59): C, 51.42; H, 6.65; N, 5.00; Found: C, 51.35; H, 6.49; N, 4.67.

G₂-[NCP(*p*-N)Ru(η⁶-*p*-cymene)Cl₂]₈ (**15**). Yellow-orange solid, yield 89.6 mg (45%). ¹H-NMR (CDCl₃): δ (ppm) = -0.09 (s, 12H, -CH₃SiCH₂CH₂CH₂Si); -0.03 (s, 48H, -(CH₃)₂SiCH₂CH₂CH₂N); 0.54 (overlapping br m, 64H, -SiCH₂CH₂CH₂Si, -CH₃SiCH₂CH₂CH₂Si and -(CH₃)₂SiCH₂CH₂CH₂N); 1.29 (overlapping br m, 72H, -SiCH₂CH₂CH₂Si, -CH₃SiCH₂CH₂CH₂Si and -(CH₃)₂CH_{cye}); 1.66 (br m, 16H, -(CH₃)₂SiCH₂CH₂CH₂N); 2.06 (s, 24H, -CH_{3cye}); 2.97 (br m, 8H, -(CH₃)₂CH_{cye}); 3.63 (br m, 16H, -(CH₃)₂SiCH₂CH₂CH₂N); 5.24 (br m, 16H, Ar_{cye}); 5.45 (br m, 16H, Ar_{cye}); 7.56 (br m, 16H, Ar); 9.05 (br m, 16H, Ar); 8.22 (br s, 8H, -CH_{imine}). ¹³C

{¹H}-NMR (CDCl₃): δ (ppm) = -4.7 (-(CH₃)₂SiCH₂CH₂CH₂N); -3.1 (-CH₃SiCH₂CH₂CH₂Si); 13.3 (-(CH₃)₂SiCH₂CH₂CH₂N); 18.4, 18.6, 19.0, 20.1 (-SiCH₂CH₂CH₂Si, -CH₃SiCH₂CH₂CH₂Si and -CH₃_{cye}); 22.5 (-(CH₃)₂CH_{cye}); 25.4 (-(CH₃)₂SiCH₂CH₂CH₂N); 30.8 (-(CH₃)₂CH_{cye}); 65.4 (-(CH₃)₂SiCH₂CH₂CH₂N); 82.3, 83.3 (-CH_{cye}); 97.5 (C_{cye}) 122.7, 144.6, 155.4 (CAr); 157.6 (-CH_{imine}). ²⁹Si-NMR (CDCl₃): δ (ppm) = -SiCH₂CH₂CH₂Si is not observed; 0.88 (-CH₃SiCH₂CH₂CH₂Si); 2.06 (-(CH₃)₂SiCH₂CH₂CH₂N). Elemental Analysis (%): Calc. For C₂₀₈H₃₃₂Cl₁₆N₁₆Ru₈Si₁₃ (4797.89): C, 52.07; H, 6.97; N, 4.67; Found: C, 52.43; H, 7.08; N, 4.75.

Chelating N,O- neutral metallodendrimers. G₀-[NCPh(*o*-O)Ru(η⁶-*p*-cymene)Cl]₁ (**19**), G₁-[NCPh(*o*-O)Ru(η⁶-*p*-cymene)Cl]₄ (**20**) and G₂-[NCPh(*o*-O)Ru(η⁶-*p*-cymene)Cl]₈ (**21**).

To a solution of *N,O*-Schiff base dendrimer (90.6 mg, 0.32 mmol of G₀-[NCPh(*o*-OH)]₁; 96.0 mg, 0.09 mmol of G₁-[NCPh(*o*-OH)]₄, 100.0 mg, 0.04 for G₂-[NCPh(*o*-OH)]₈) in dry ethanol, was added triethylamine (34.60 mg, 0.36 mmol for G₀-[NCPh(*o*-OH)]₁; 36.95 mg, 0.36 mmol for G₁-[NCPh(*o*-OH)]₄; 34.63 mg, 0.34 mmol for G₂-[NCPh(*o*-OH)]₈). The yellow suspension was stirred at room temperature for 30 mins. Immediately, [Ru(η⁶-*p*-cymene)Cl₂]₂ (101 mg, 0.16 mmol for G₀-[NCPh(*o*-O)Ru(η⁶-*p*-cymene)Cl]₁ (**19**); 109 mg, 0.18 mmol for G₁-[NCPh(*o*-O)Ru(η⁶-*p*-cymene)Cl]₄ (**20**) and 99.2 mg, 0.16 mmol for G₂-[NCPh(*o*-O)Ru(η⁶-*p*-cymene)Cl]₈ (**21**) was added to the reaction mixture and allowed to stir overnight at room temperature. The solvent was evaporated under reduced pressure and the resulting solid was purified by an extraction of CH₂Cl₂/H₂O. Then, the organic phase was dried over MgSO₄ and the solution was filtered and evaporated. The G₁-[NCPh(*o*-

O)Ru(η^6 -*p*-cymene)Cl]₄ and G₂-[NCPh(*o*-O)Ru(η^6 -*p*-cymene)Cl]₈ complexes were purified by sized exclusion chromatography.

G₀-[NCPh(*o*-O)Ru(η^6 -*p*-cymene)Cl]₁ (**19**). Brown solid, 144 mg (81%). ¹H-NMR (CDCl₃): δ (ppm) = 0.56 (overlapping m, 8H, -Si(CH₂CH₃)₃ and -SiCH₂CH₂); 0.95 (m, 9H, -Si(CH₂CH₃)₃); 1.12 (d, ³J (*H-H*) = 6.9 Hz, 3H, -(CH₃)₂CH_{cye}); 1.23 (d, ³J (*H-H*) = 6.9 Hz, 3H, -(CH₃)₂CH_{cye}); 1.83 (br m, 1H, -SiCH₂CH₂CH₂N); 2.07 (br m, 1H, -SiCH₂CH₂CH₂N); 2.19 (s, 3H, -CH_{3cye}); 2.77 (m, 1H, -(CH₃)₂CH_{cye}); 4.00 (br m, 1H, -SiCH₂CH₂CH₂N); 4.20 (br m, 1H, -SiCH₂CH₂CH₂N); 5.01 (m, 1H, Ar_{cye}); 5.37 (m, 3H, Ar_{cye}); 6.39 (m, 1H, Ar); 6.92 (m, 2H, Ar); 7.13 (m, 1H, Ar); 7.66 (s, 1H, -CH_{imine}). ¹³C {¹H}-NMR (CDCl₃): δ (ppm) = 3.3 (-Si(CH₂CH₃)₃); 7.6 (-Si(CH₂CH₃)₃); 9.1 (-SiCH₂CH₂); 18.6 (-CH_{3cye}); 21.8, 22.9 (-(CH₃)₂CH_{cye}); 26.0 (-SiCH₂CH₂CH₂N); 30.6 (-(CH₃)₂CH_{cye}); 73.1 (-SiCH₂CH₂CH₂N); 80.2, 82.1, 83.2, 85.9 (-CH_{cye}); 97.4, 101.6 (C_{cye}); 114.1, 119.3, 122.4, 134.4, 134.6, 163.4 (CAr); 165.0 (-CH_{imine}). ²⁹Si-NMR (CDCl₃): δ (ppm) = 7.10 (-Si(CH₂CH₃)₃). Elemental Analysis (%): Calc. For C₂₆H₄₀ClNORuSi (547.24): C, 57.07; H, 7.37; N, 2.56; Found: C, 57.39; H, 7.20; N, 2.83.

G₁-[NCPh(*o*-O)Ru(η^6 -*p*-cymene)Cl]₄ (**20**). Brown solid, yield 136 mg (70%). ¹H-NMR (CDCl₃): δ (ppm) = 0.01 (br s, 24H, -(CH₃)₂SiCH₂CH₂CH₂N); 0.59 (overlapping m, 24H, -SiCH₂CH₂CH₂Si and -SiCH₂CH₂CH₂N); 1.10 (m, 12H, -(CH₃)₂CH_{cye}); 1.23 (m, 12H, -(CH₃)₂CH_{cye}); 1.28 (br m, 8H, -SiCH₂CH₂CH₂Si); 1.82 (br m, 4H, -SiCH₂CH₂CH₂N); 2.03 (br m, 4H, -SiCH₂CH₂CH₂N); 2.19 (s, 12H, -CH_{3cye}); 2.74 (br s, 4H, -(CH₃)₂CH_{cye}); 3.96 (br m, 4H, -SiCH₂CH₂CH₂N); 4.24 (br m, 4H, -SiCH₂CH₂CH₂N); 5.01 (m, 4H, Ar_{cye}); 5.38 (m, 12H, Ar_{cye}); 6.40 (m, 4H, Ar); 6.92 (m, 8H, Ar); 7.12 (m, 4H, Ar); 7.66 (s, 4H, -CH_{imine}). ¹³C {¹H}-NMR

(CDCl₃): δ (ppm) = -3.1 (-(CH₃)₂SiCH₂CH₂CH₂N); 13.0 (-SiCH₂CH₂CH₂N); 17.6, 18.6, 18.7 (-SiCH₂CH₂CH₂Si and -CH₃_{cye}); 21.7, 22.9 (-(CH₃)₂CH_{cye}); 25.9 (-SiCH₂CH₂CH₂N); 30.6 (-(CH₃)₂CH_{cye}); 73.0 (-SiCH₂CH₂CH₂N); 80.2, 82.2, 83.4, 86.1 (-CH_{cye}); 97.3, 101.5 (C_{cye}); 114.1, 119.3, 122.3, 134.6, 163.3 (CAr); 164.9 (-CH_{imine}). ²⁹Si-NMR (CDCl₃): δ (ppm) = 0.60 (-SiCH₂CH₂CH₂Si); 2.01 (-(CH₃)₂SiCH₂CH₂CH₂N). Elemental Analysis (%): Calc. For C₁₀₀H₁₄₈Cl₄N₄O₄Ru₄Si₅ (2156.79): C, 55.59; H, 6.62; N, 2.70; Found: C, 55.93; H, 6.89; N, 2.58.

G₂-[NCPPh(*o*-O)Ru(η^6 -*p*-cymene)Cl]₈ (**21**). Brown-red solid, yield 126 mg (68%). ¹H-NMR (CDCl₃): δ (ppm) = -0.06 (br s, 48H, -(CH₃)₂SiCH₂CH₂CH₂N); 0.02 (br s, 12H, -CH₃SiCH₂CH₂CH₂Si); 0.57 (overlapping br m, 64H, -SiCH₂CH₂CH₂Si, -CH₃SiCH₂CH₂CH₂Si and -(CH₃)₂SiCH₂CH₂CH₂N); 1.10 (br m, 24H, -(CH₃)₂CH_{cye}); 1.25 (overlapping br m, 72H, -SiCH₂CH₂CH₂Si, -CH₃SiCH₂CH₂CH₂Si and -(CH₃)₂CH_{cye}); 1.82 (br m, 8H, -(CH₃)₂SiCH₂CH₂CH₂N); 2.03 (br m, 8H, -(CH₃)₂SiCH₂CH₂CH₂N); 2.19 (s, 24H, -CH₃_{cye}); 2.75 (br s, 8H, -(CH₃)₂CH_{cye}); 3.94 (br m, 8H, -SiCH₂CH₂CH₂N); 4.23 (br m, 8H, -SiCH₂CH₂CH₂N); 5.00 (m, 8H, Ar_{cye}); 5.38 (m, 24H, Ar_{cye}); 6.39 (br s, 8H, Ar); 6.91 (overlapping m, 16H, Ar); 7.13 (br s, 8H, Ar); 7.66 (s, 8H, -CH_{imine}). ¹³C{¹H}-NMR (CDCl₃): δ (ppm) = -4.7 (-(CH₃)₂SiCH₂CH₂CH₂N); -3.0 (-CH₃SiCH₂CH₂CH₂Si); 13.1 (-(CH₃)₂SiCH₂CH₂CH₂N); 17.9, 18.6, 18.8, 19.0, 19.3, 20.2, 21.8 (-SiCH₂CH₂CH₂Si, -CH₃SiCH₂CH₂CH₂Si and -CH₃_{cye}); 23.0, 25.9 (-(CH₃)₂CH_{cye}); 29.8 (-(CH₃)₂SiCH₂CH₂CH₂N); 30.7 (-(CH₃)₂CH_{cye}); 73.1 (-(CH₃)₂SiCH₂CH₂CH₂N); 80.2, 82.3, 83.5, 86.2 (-CH_{cye}); 97.3, 101.6 (C_{cye}); 114.1, 119.4, 122.4, 134.6, 163.4 (CAr); 165.1 (-CH_{imine}). ²⁹Si-NMR (CDCl₃): δ (ppm) = -SiCH₂CH₂CH₂Si is not observed; 0.90 (-(CH₃)₂SiCH₂CH₂CH₂Si); 2.16

(CH₃SiCH₂CH₂CH₂N). Elemental Analysis (%): Calc. For C₂₁₆H₃₃₂Cl₈N₈O₈Ru₈Si₁₃
(4626.29): C, 56.08; H, 7.23; N, 2.42; Found: C, 56.59; H, 7.66; N, 2.44.

3. Selected ^1H NMR and ^{13}C NMR spectra of dendritic ligands (**1-9**)

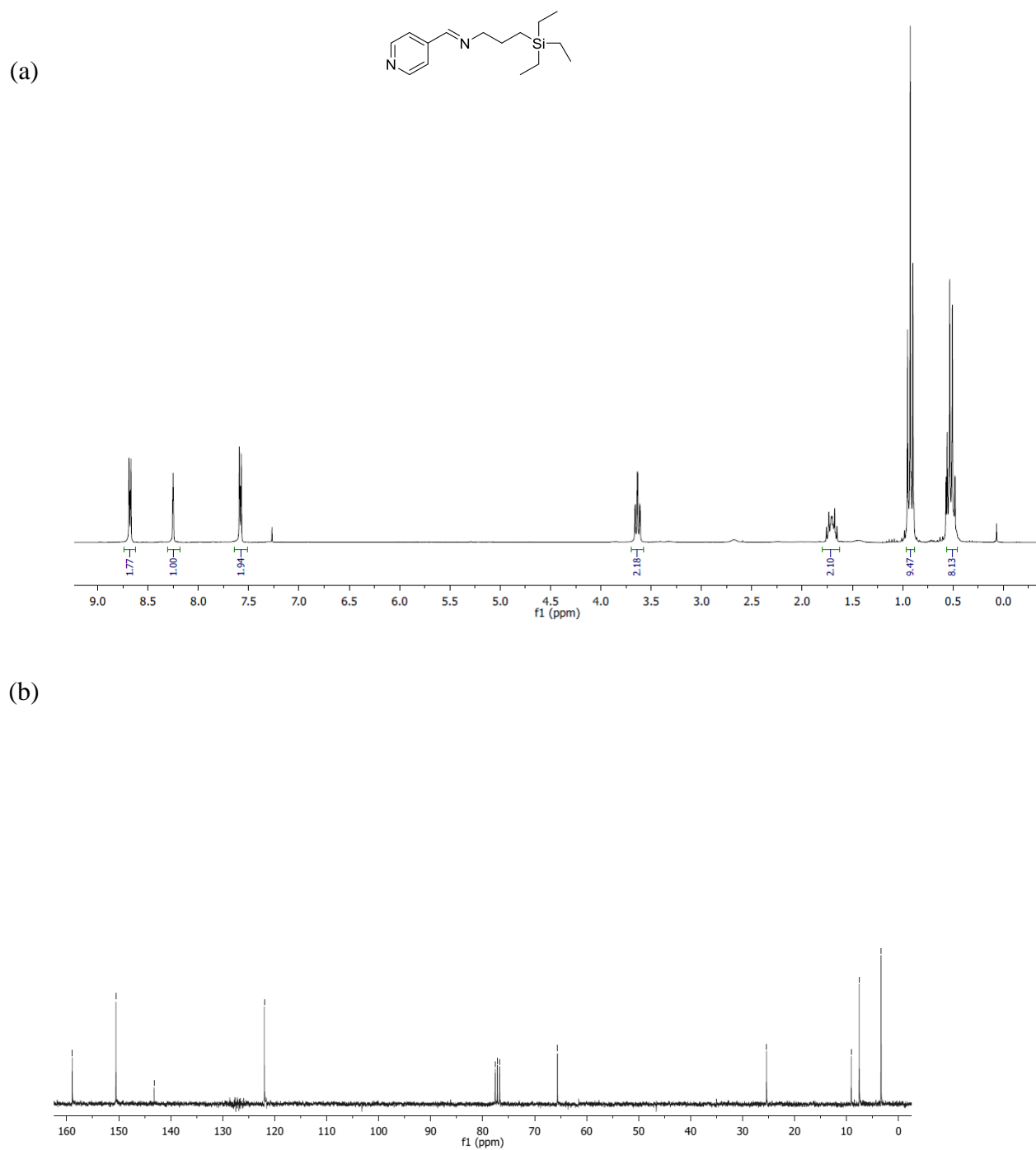
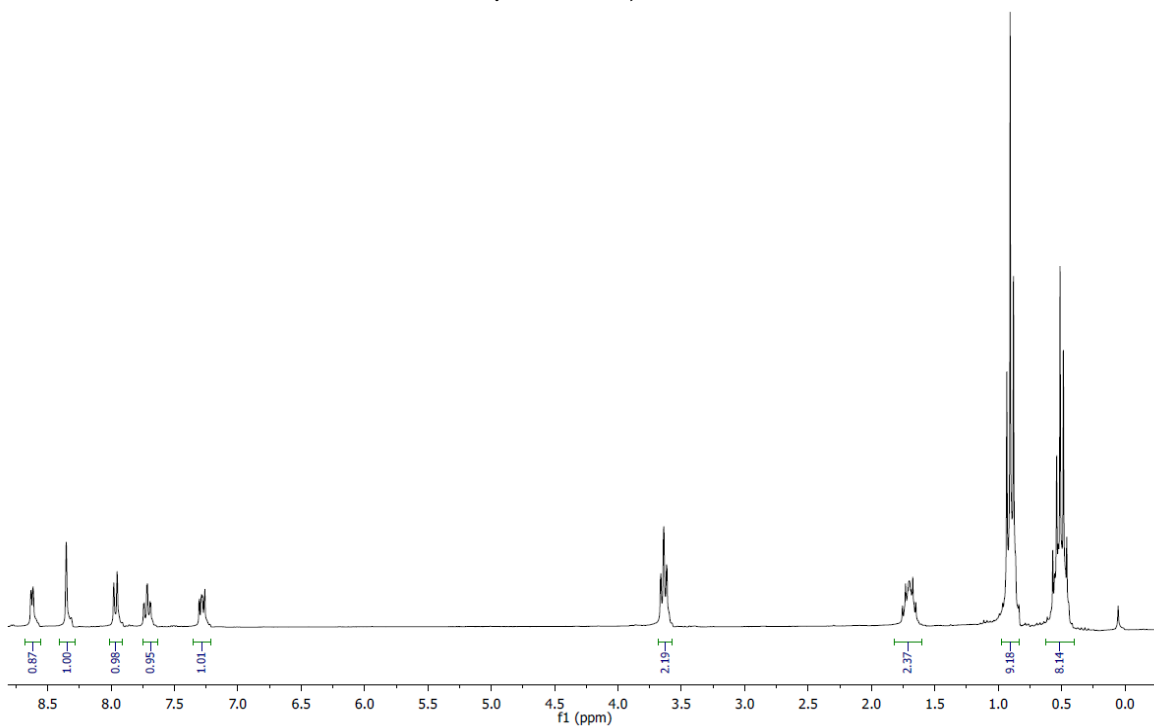
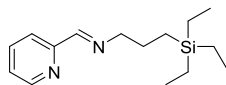


Fig. S1 a) ^1H -NMR (300 MHz, CDCl_3) and b) ^{13}C $\{^1\text{H}\}$ -NMR (300 MHz, CDCl_3) spectra of compound $\text{G}_0\text{-[NCPH}(p\text{-N})]_1$ (**1**).

(a)



(b)

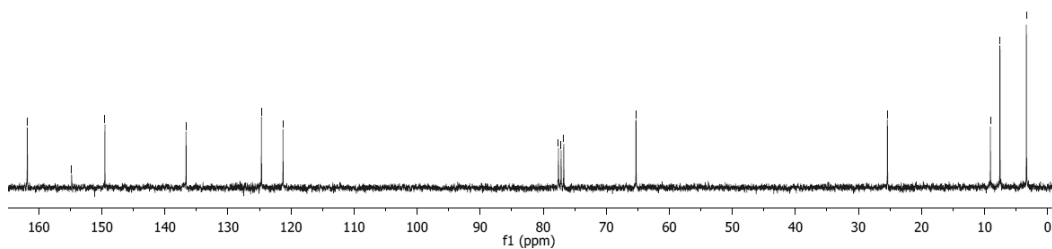
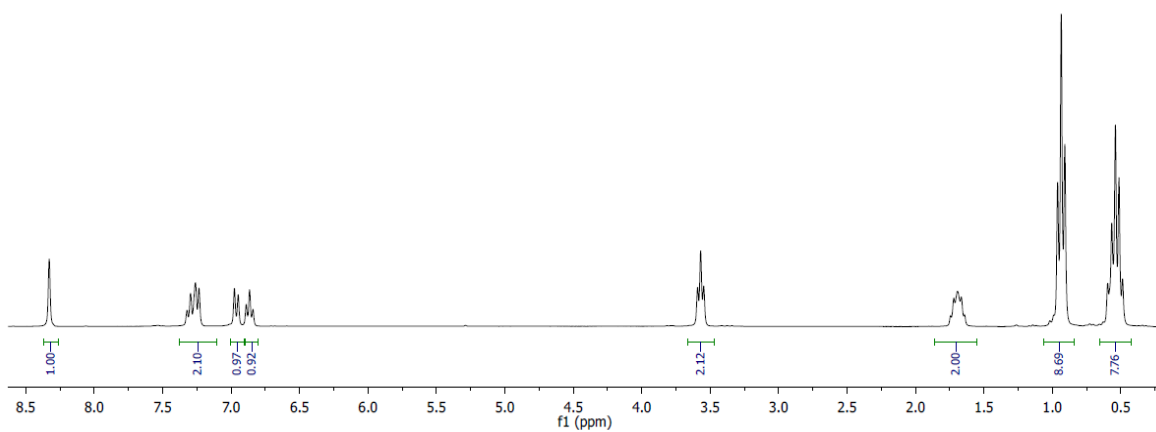
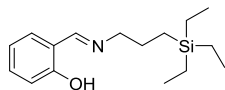


Fig. S2 a) ¹H-NMR (300 MHz, CDCl₃) and b) ¹³C {¹H}-NMR (300 MHz, CDCl₃) spectra of compound G₀-[NCPH(*o*-N)]₁ (**4**).

(a)



(b)

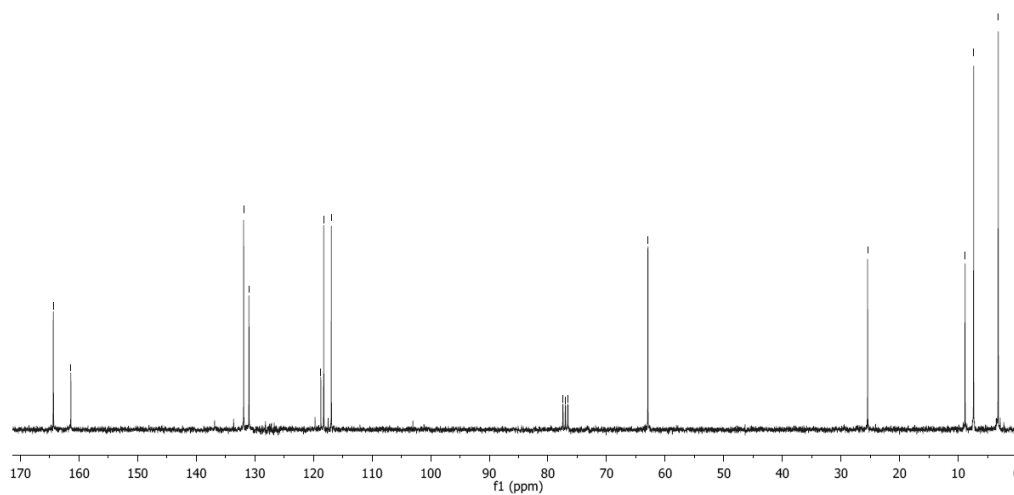
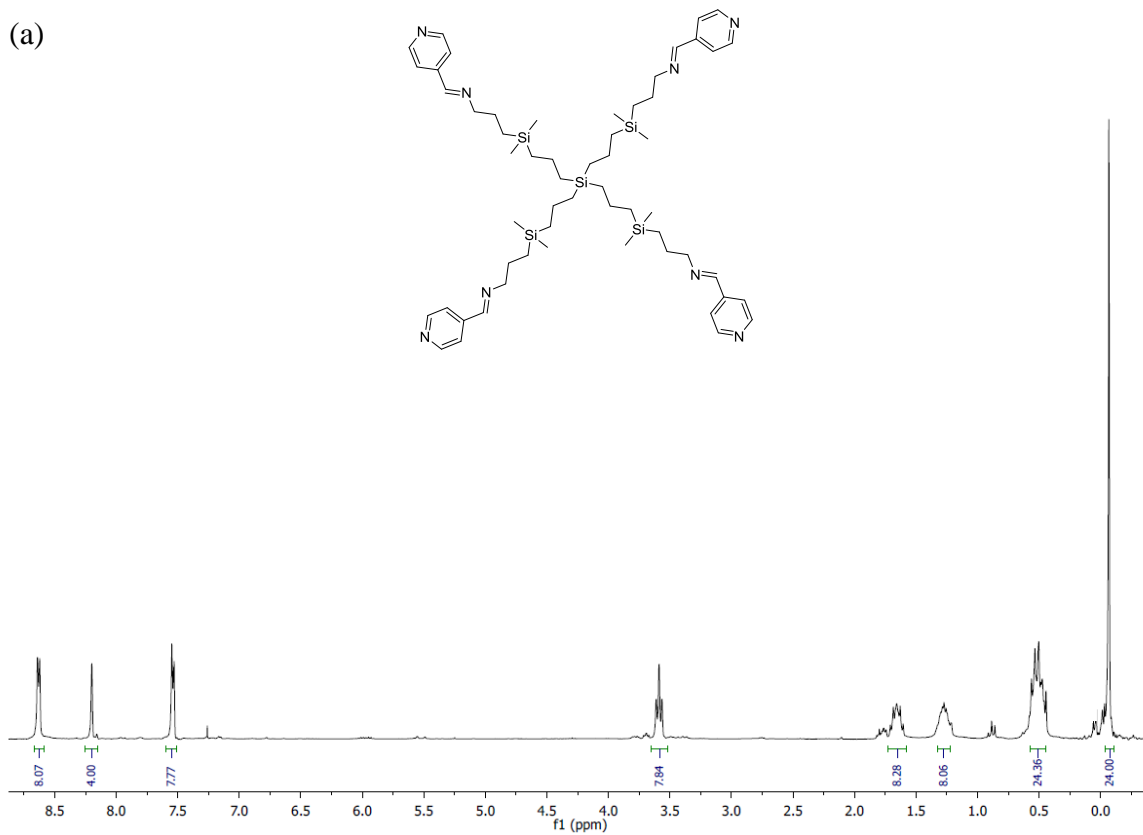


Fig. S3 a) ¹H-NMR (300 MHz, CDCl₃) and b) ¹³C {¹H}-NMR (300 MHz, CDCl₃) spectra of compound G₀-[NCPH(*o*-OH)]₁ (**7**).

(a)



(b)

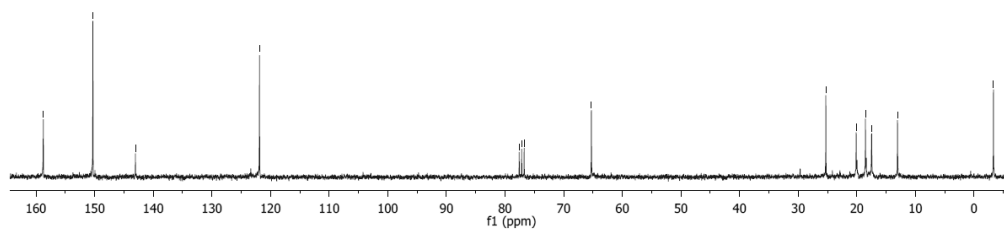
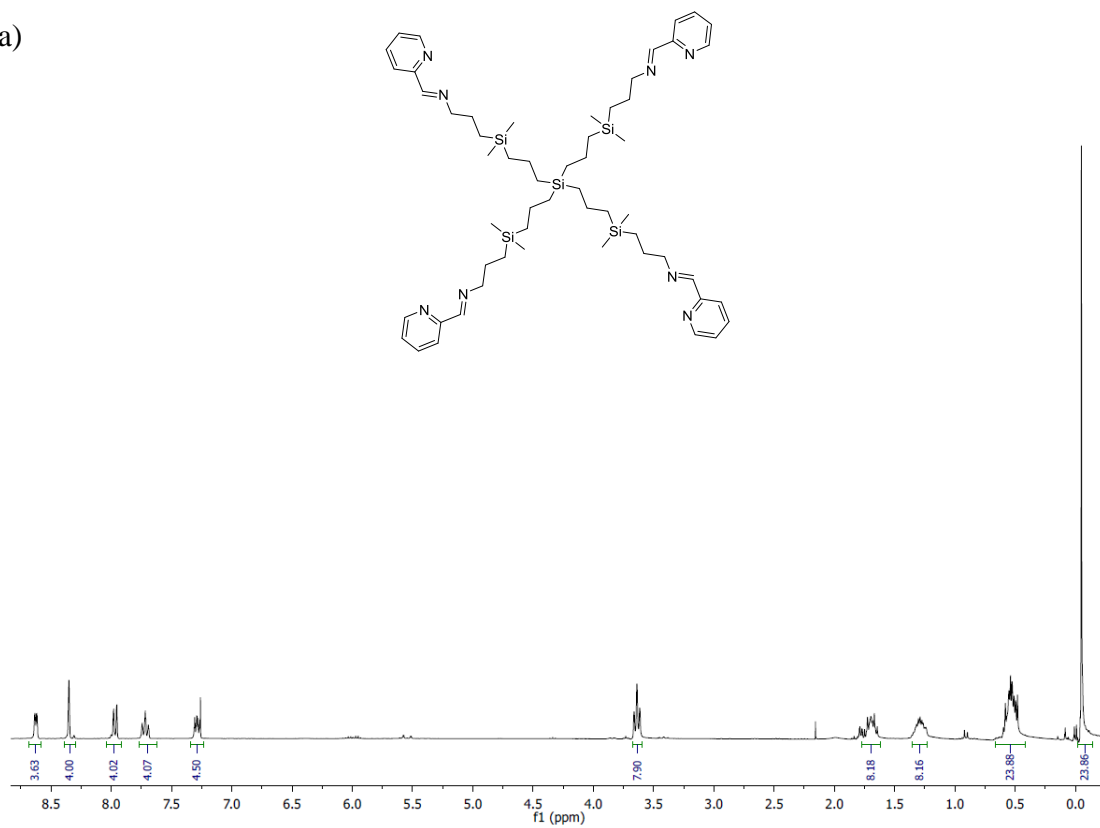


Fig. S4 a) $^1\text{H-NMR}$ (300 MHz, CDCl_3) and b) $^{13}\text{C} \{^1\text{H}\}$ -NMR (300 MHz, CDCl_3) spectra of compound G_7 -[NCPH(*p*-N)]₄ (**2**).

(a)



(b)

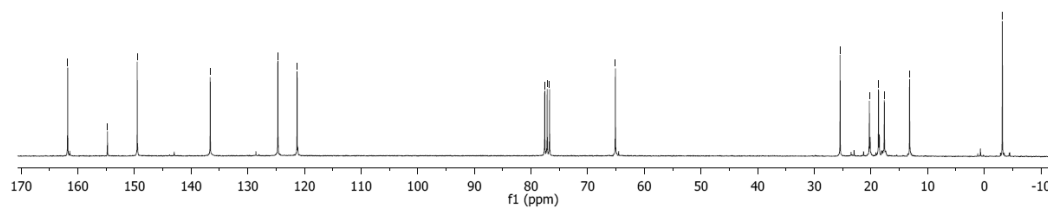


Fig. S5 a) ¹H-NMR (300 MHz, CDCl₃) and b) ¹³C {¹H}-NMR (300 MHz, CDCl₃) spectra of compound G₁-[NCPH(*o*-N)]₄ (**5**).

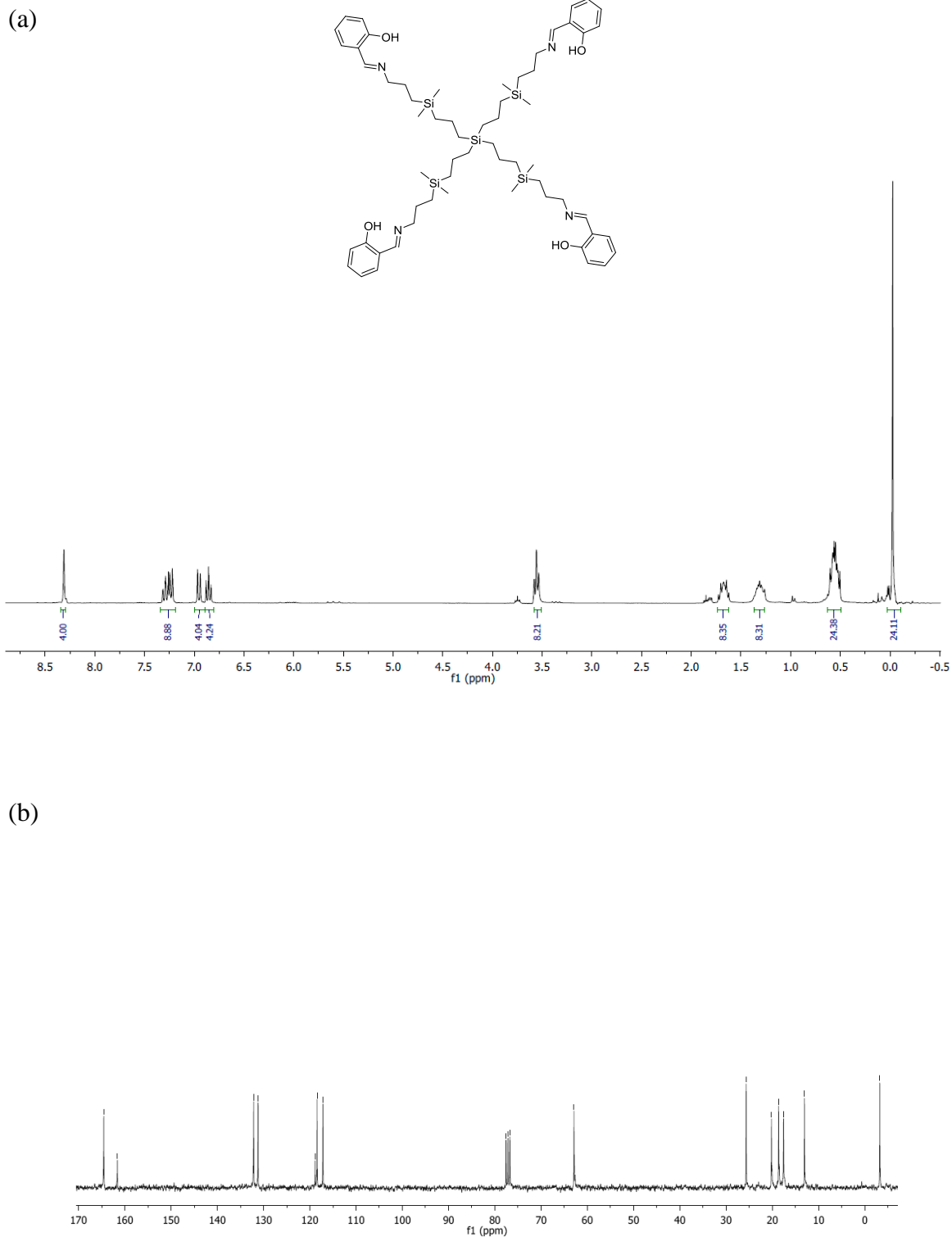
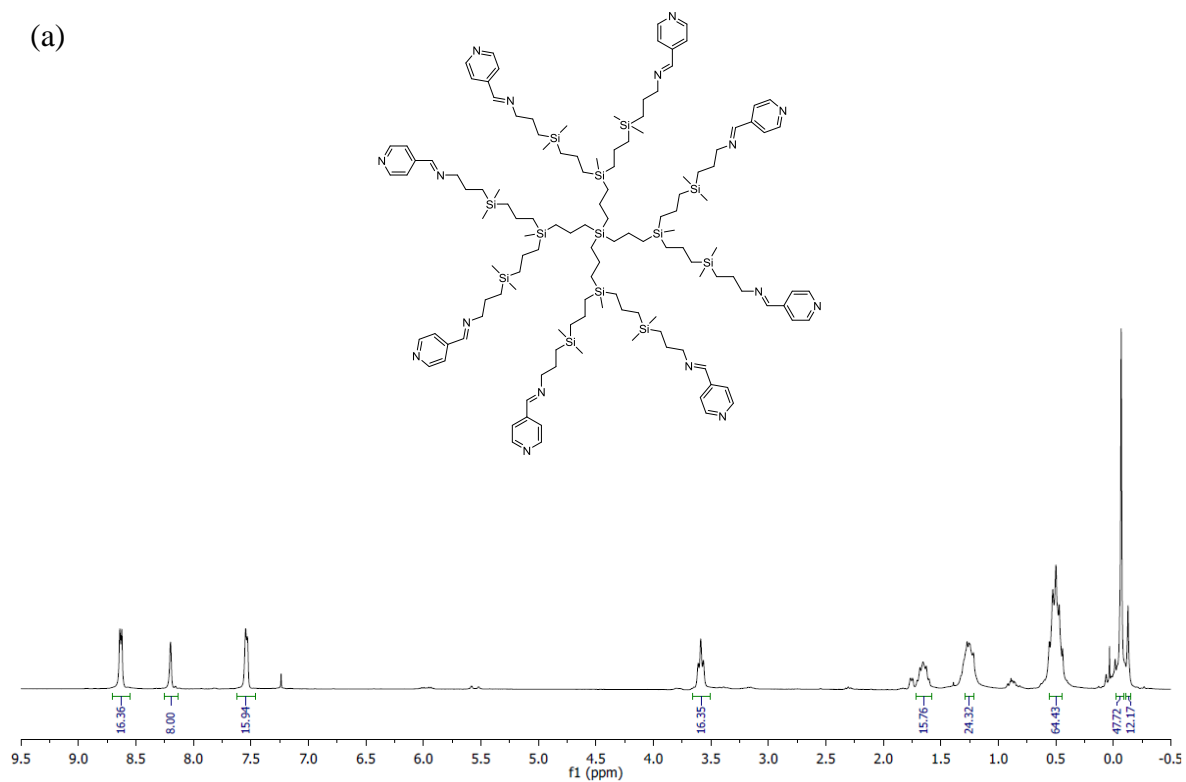


Fig. S6 a) ^1H -NMR (300 MHz, CDCl_3) and b) ^{13}C $\{^1\text{H}\}$ -NMR (300 MHz, CDCl_3) spectra of compound G_1 -[NCP(*o*-OH)]₄ (**8**).

(a)



(b)

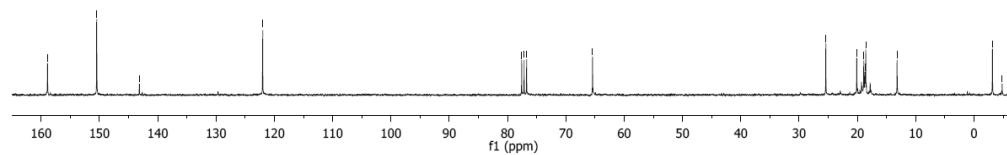


Fig. S7 a) ¹H-NMR (300 MHz, CDCl₃) and b) ¹³C {¹H}-NMR (300 MHz, CDCl₃) spectra of compound G₂-[NCPH(*p*-N)]₈ (**3**).

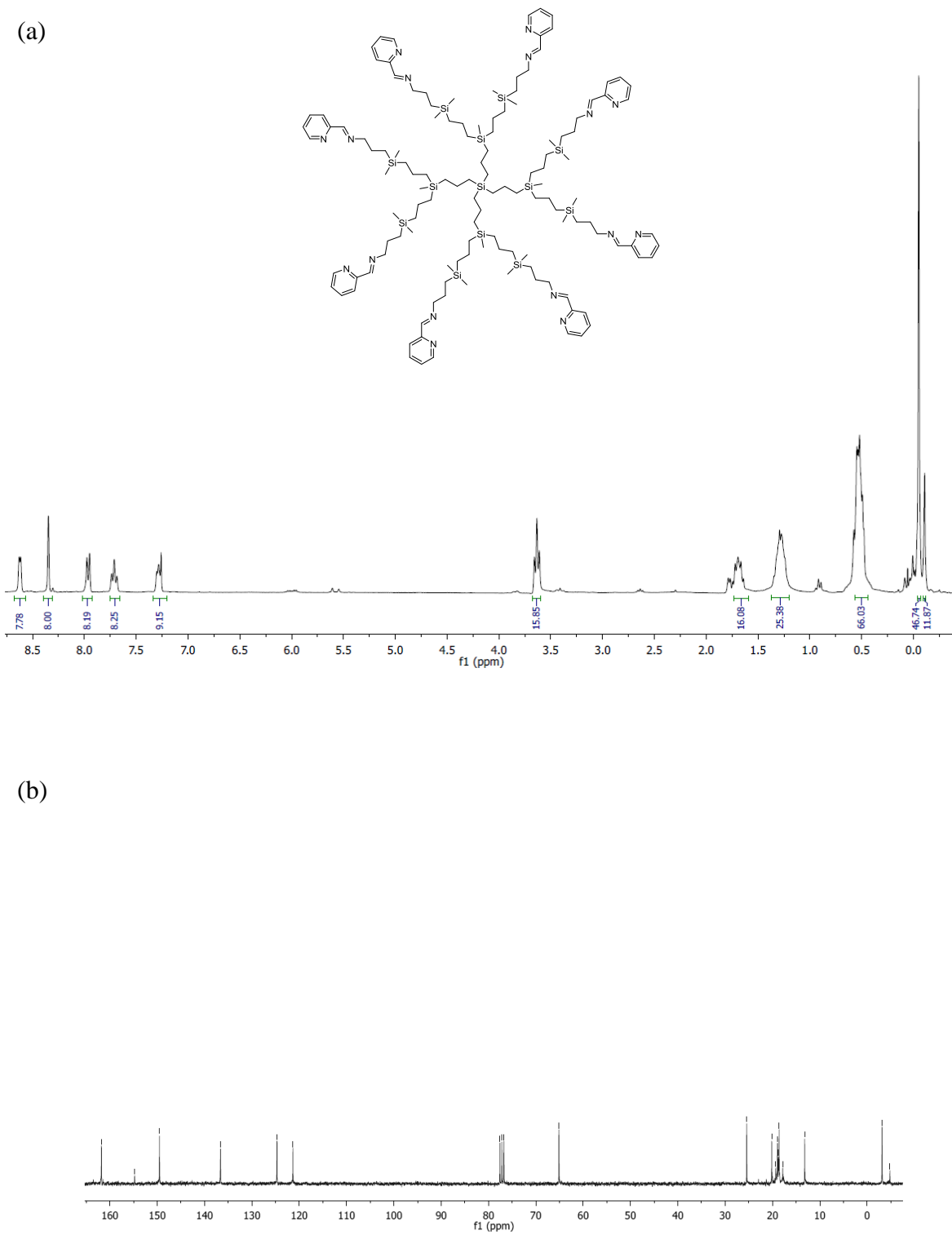
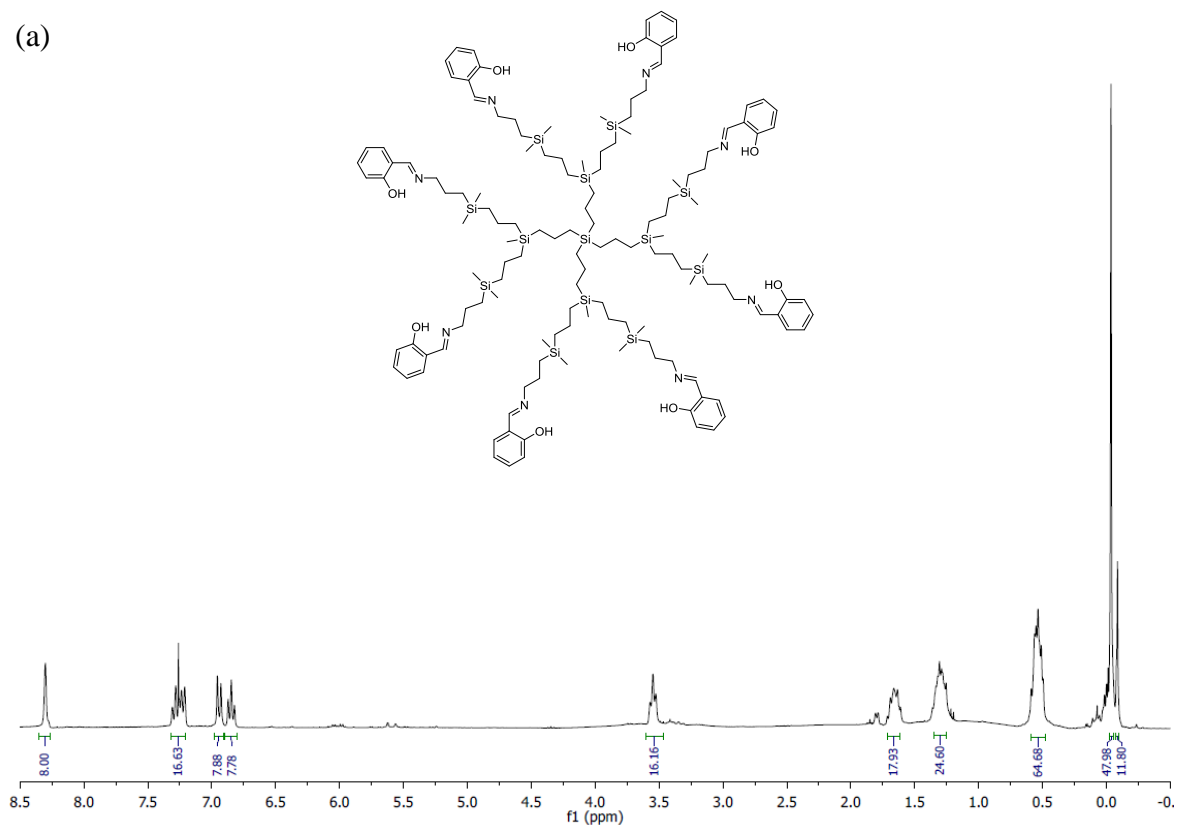


Fig. S8 a) ^1H -NMR (300 MHz, CDCl_3) and b) ^{13}C $\{^1\text{H}\}$ -NMR (300 MHz, CDCl_3) spectra of compound $\text{G}_2\text{-[NCPH}(o\text{-N})]_8$ (**6**).

(a)



(b)

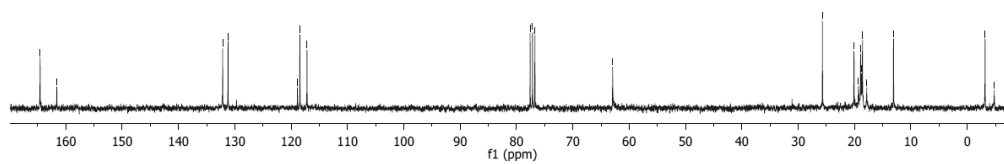


Fig. S9 a) ¹H-NMR (300 MHz, CDCl₃) and b) ¹³C {¹H}-NMR (300 MHz, CDCl₃) spectra of compound G₂-[NCPH(*o*-OH)]₈ (**9**).

4. Selected ^1H NMR and ^{13}C NMR spectra of carbosilane metallodendrimers based on arene ruthenium (II) complexes (**10**, **11**, **13-15**, **17,18**)

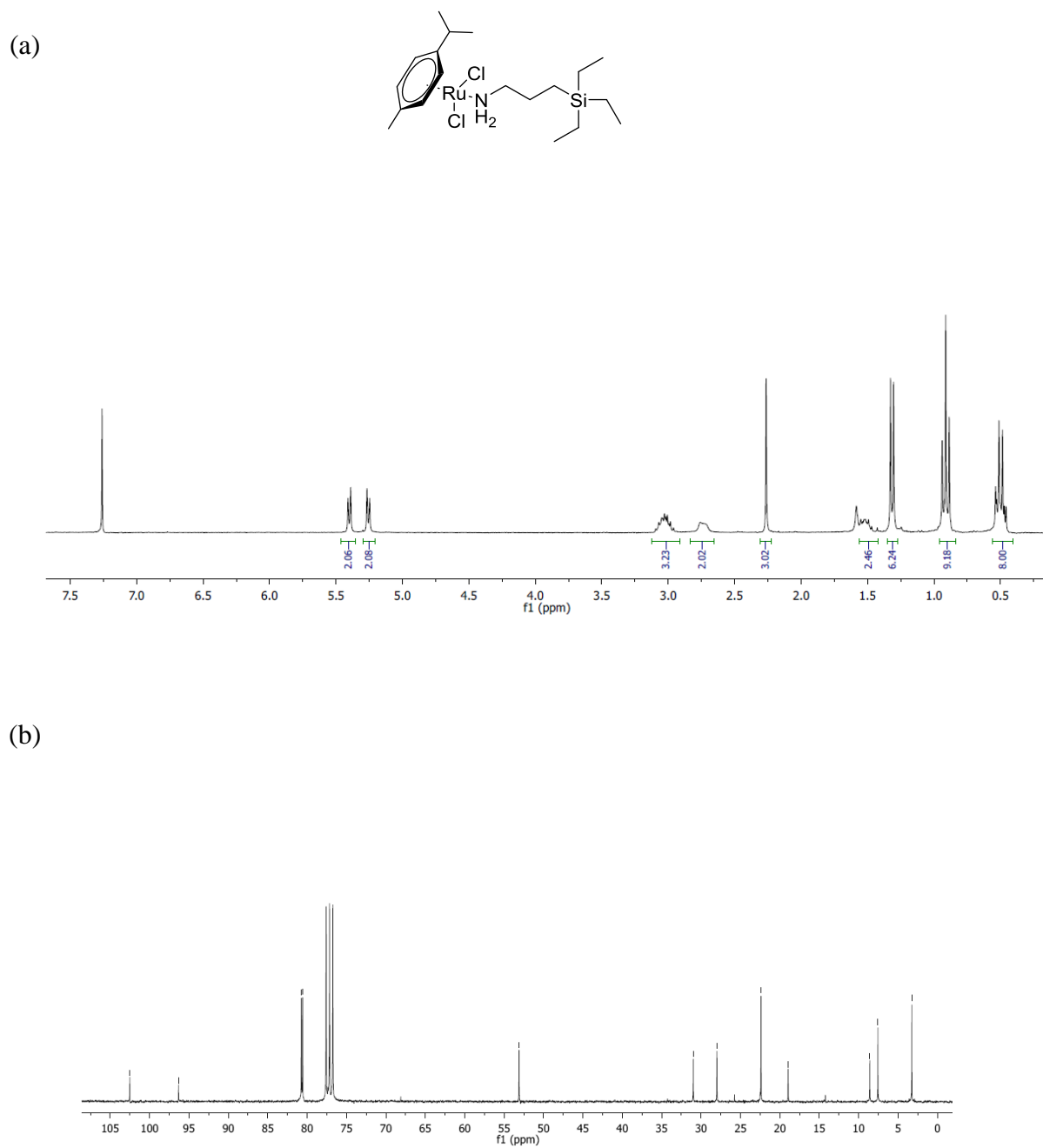


Fig. S10 a) ^1H -NMR (300 MHz, CDCl₃) and b) ^{13}C $\{^1\text{H}\}$ -NMR (300 MHz, CDCl₃) spectra of compound $\text{G}_0\text{-}[\text{NH}_2\text{Ru}(\eta^6\text{-}p\text{-cymene})\text{Cl}_2]_1$ (**10**).

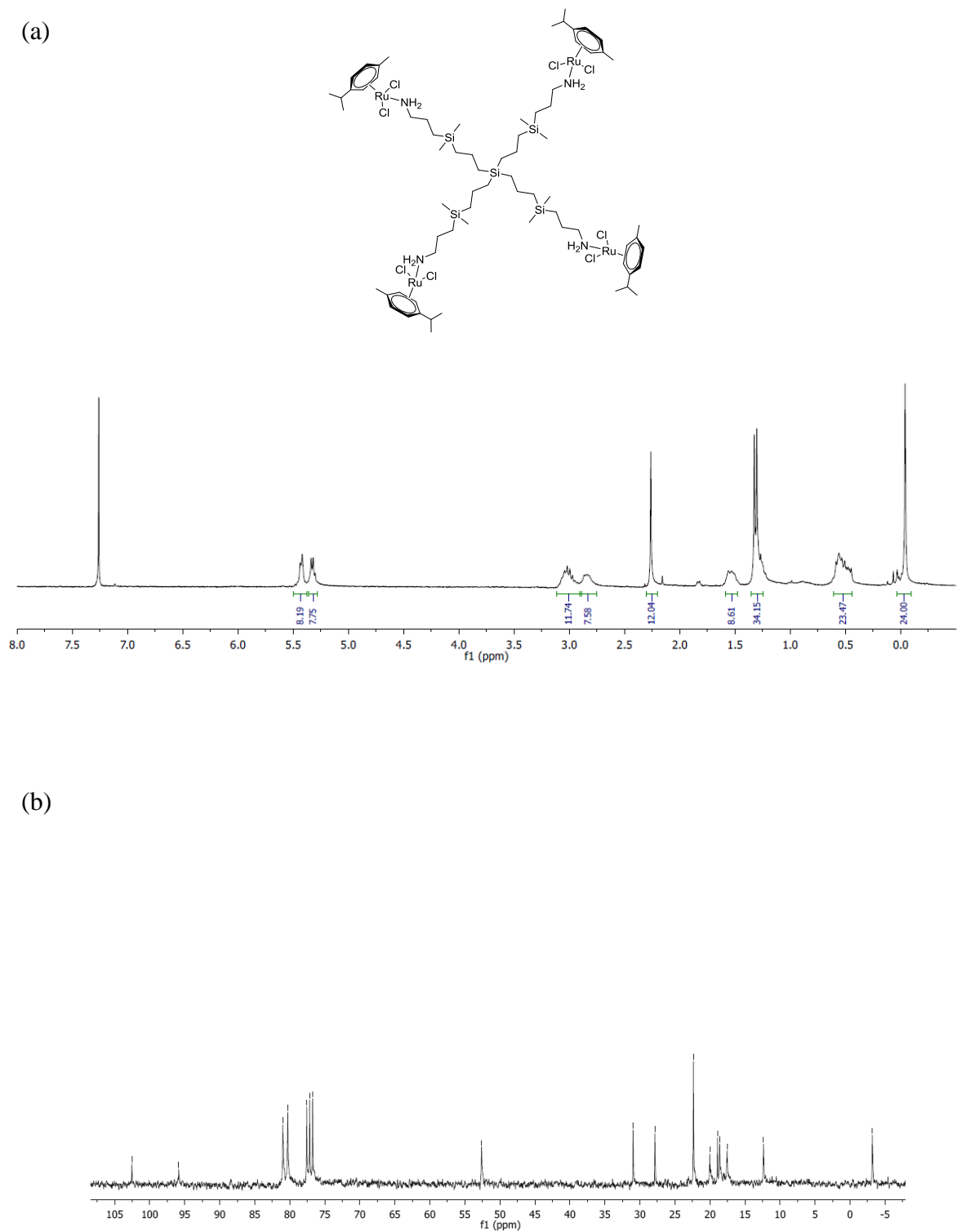
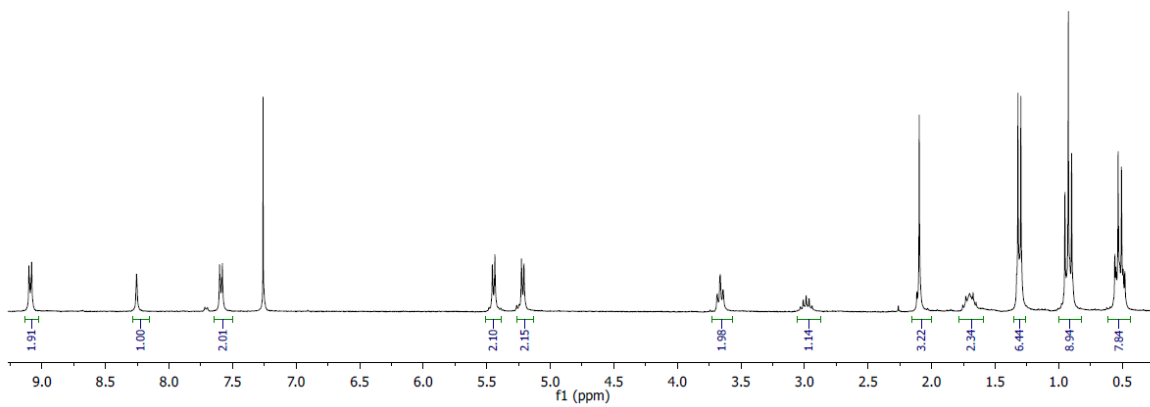
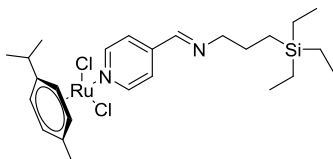


Fig. S11 a) ^1H -NMR (300 MHz, CDCl_3) and b) ^{13}C $\{^1\text{H}\}$ -NMR (300 MHz, CDCl_3) spectra of compound G_7 - $[\text{NH}_2\text{Ru}(\eta^6\text{-}p\text{-cymene})\text{Cl}_2]_4$ (**11**).

(a)



(b)

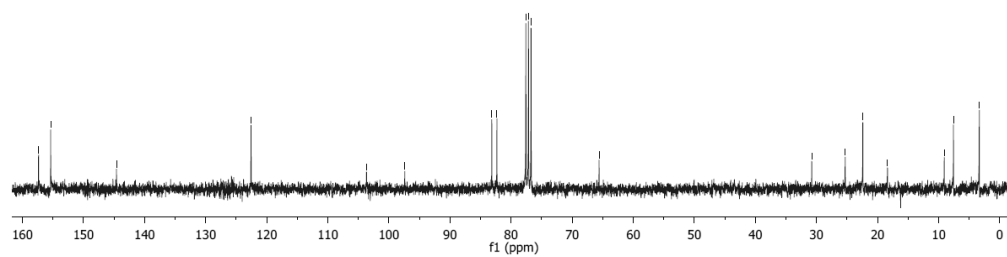


Fig. S12 a) ^1H -NMR and b) ^{13}C $\{^1\text{H}\}$ -NMR spectra of compound $\text{G}_0\text{-}[\text{NCPH}(p\text{-N})\text{Ru}(\eta^6\text{-}p\text{-cymene})\text{Cl}_2]_I$ (**13**).

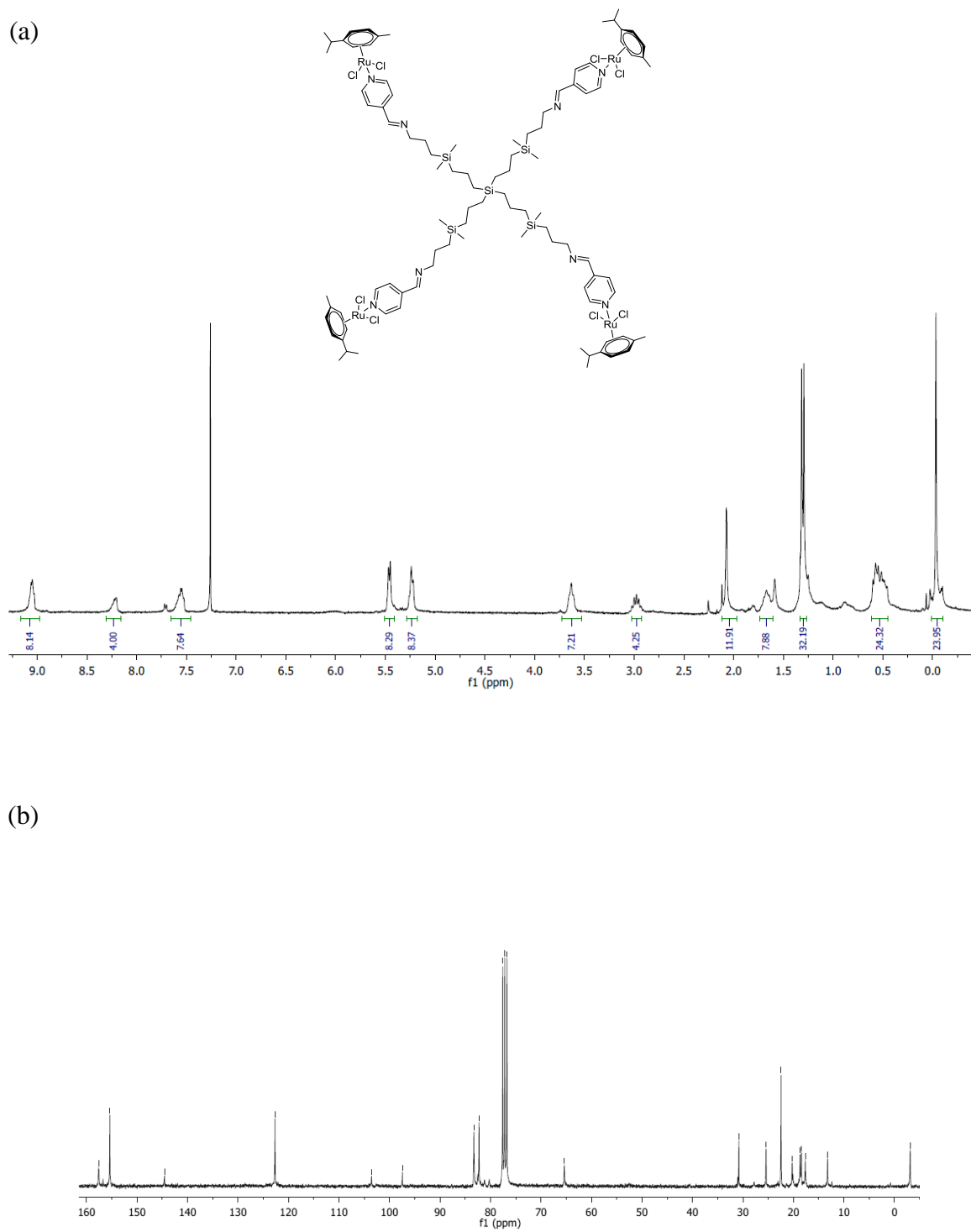
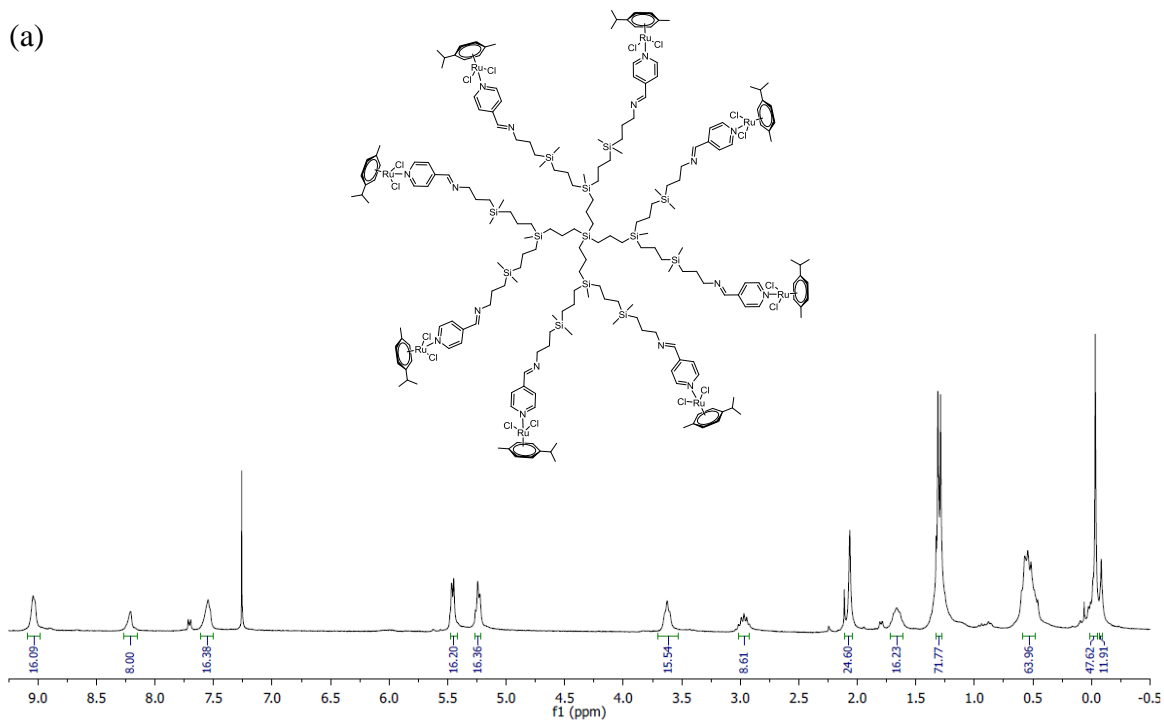


Fig. S13 a) ^1H -NMR and b) ^{13}C $\{^1\text{H}\}$ -NMR spectra of compound G_1 -[NCP h (p -N)Ru(η^6 - p -cymene)Cl $_2$] $_4$ (**14**).

(a)



(b)

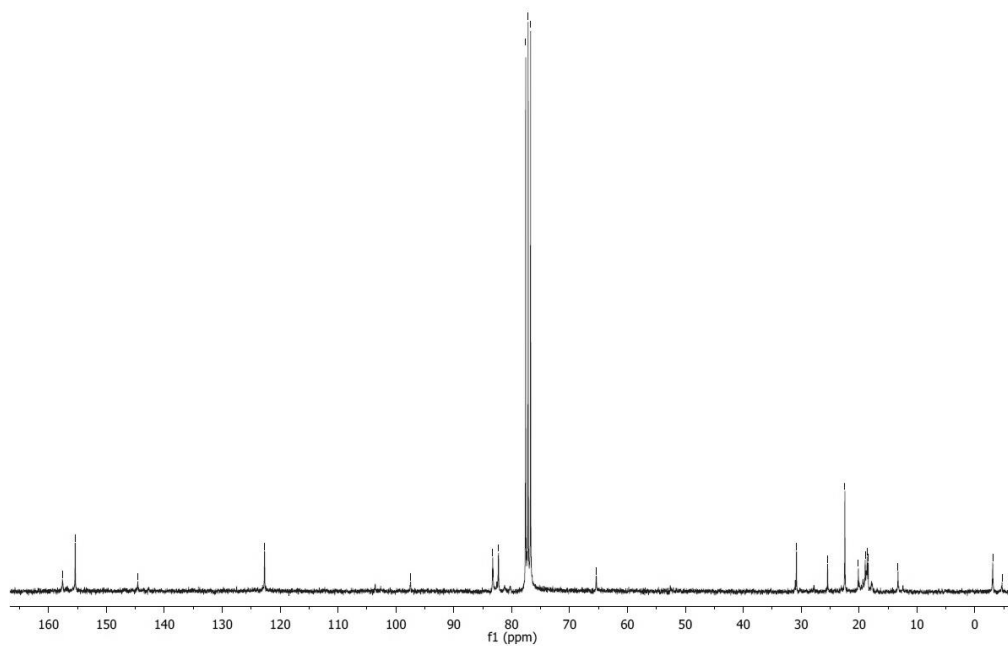


Fig. S14 a) ¹H-NMR (300 MHz, CDCl₃) and b) ¹³C {¹H}-NMR (300 MHz, CDCl₃) spectra of compound G₂-[NCPH(*p*-N)Ru(η⁶-*p*-cymene)Cl₂]₈ (**15**).

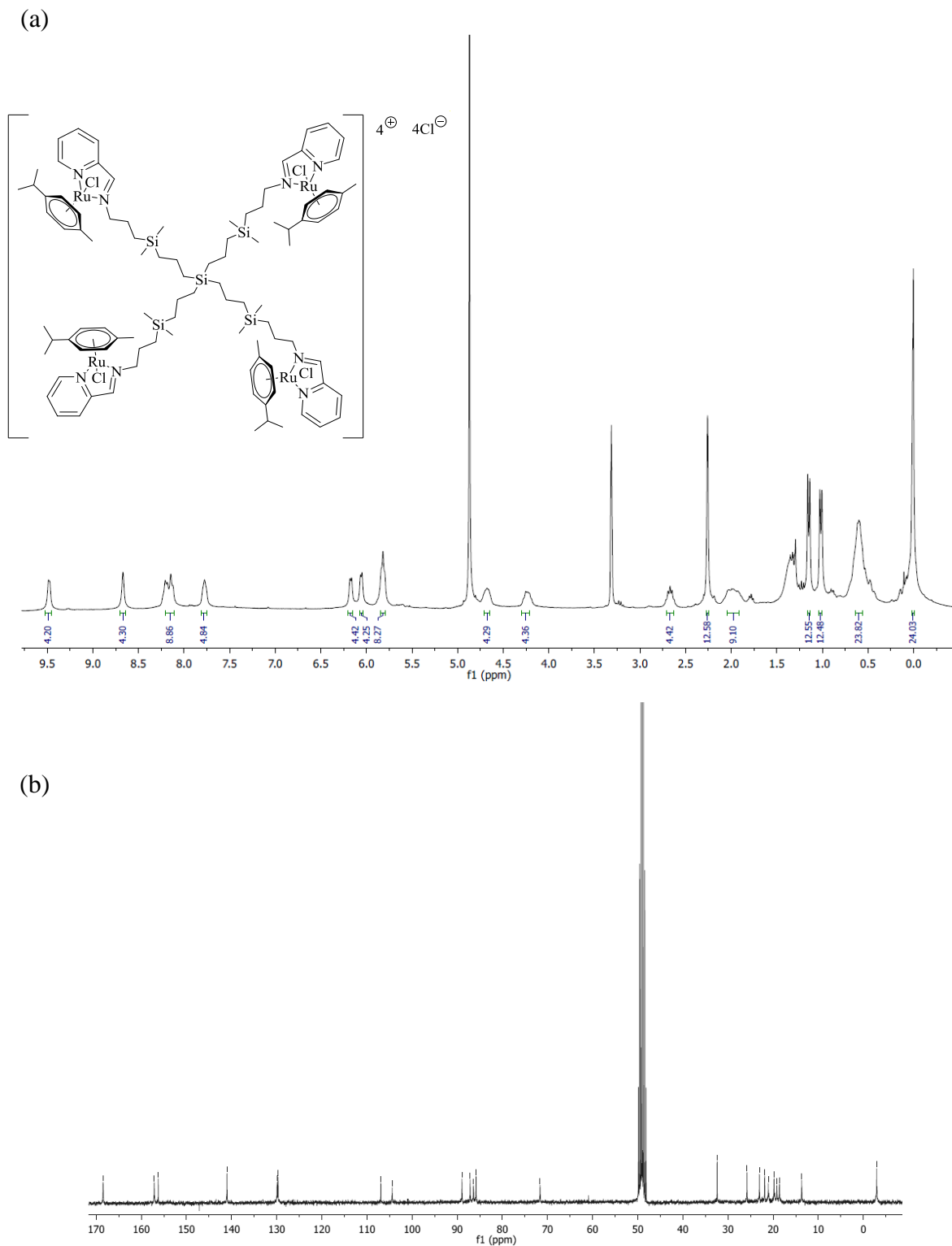


Fig. S15 a) ^1H -NMR (300 MHz, CD_3OD) and b) ^{13}C $\{^1\text{H}\}$ -NMR (300 MHz, CD_3OD) spectra of compound G_I - $[[\text{NCP}h(o\text{-N})\text{Ru}(\eta^6\text{-}p\text{-cymene})\text{Cl}]\text{Cl}]_4$ (**17**).

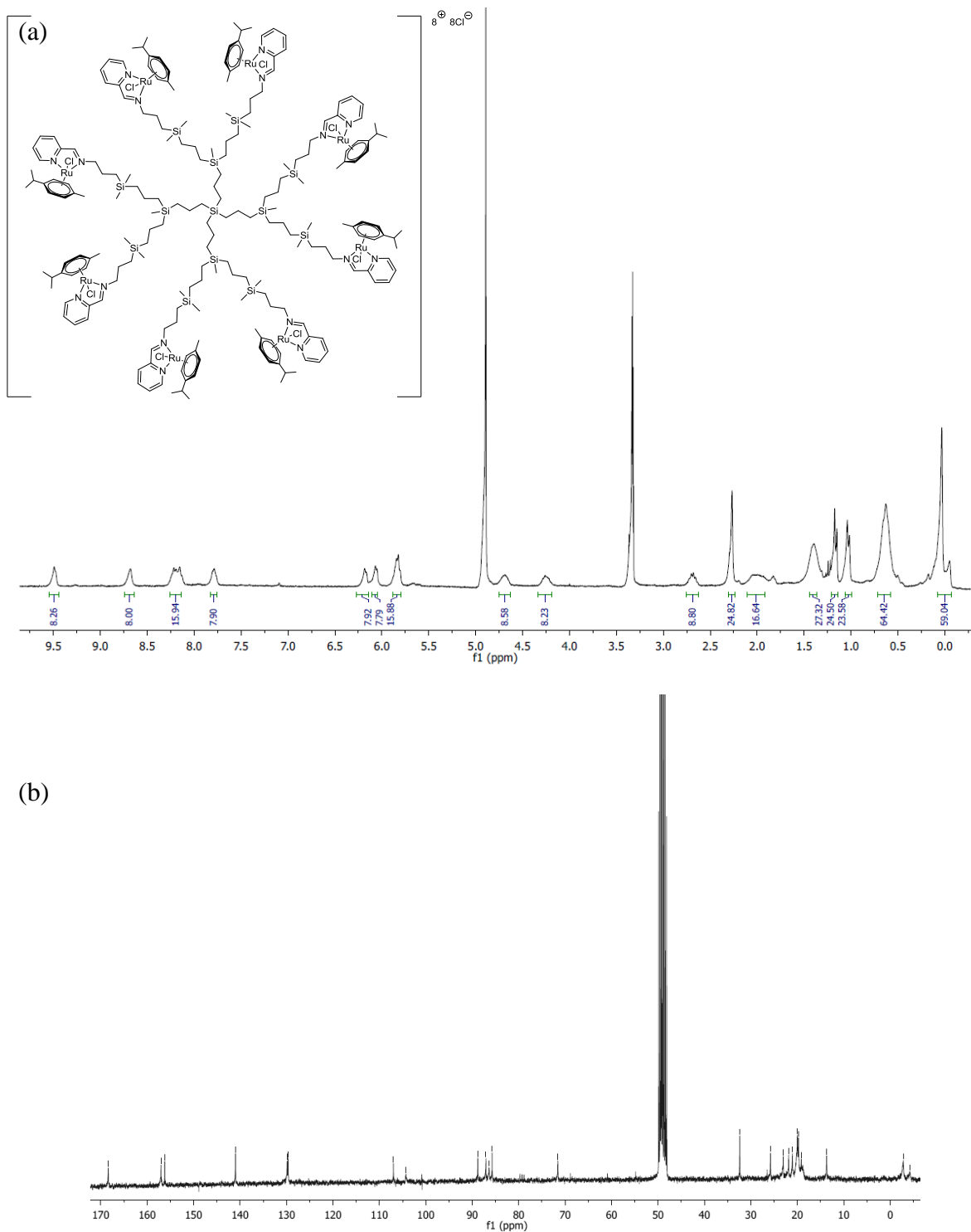
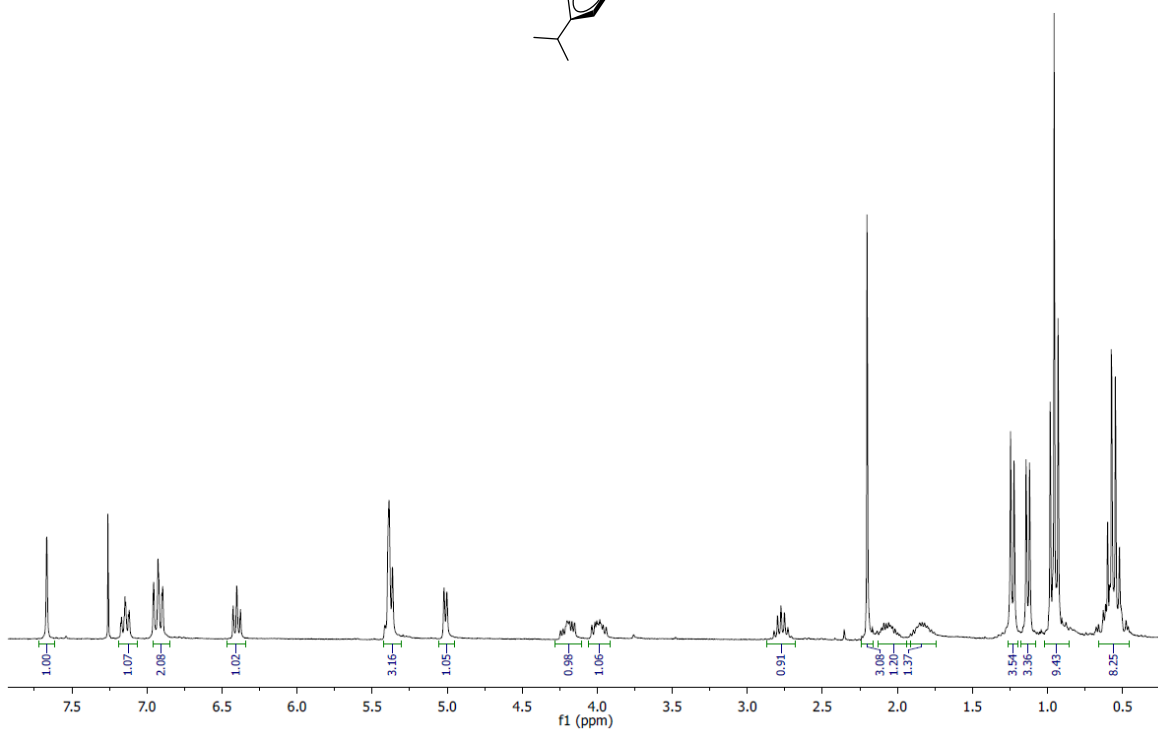
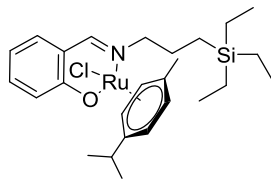


Fig. S16 a) ^1H -NMR (300 MHz, CD_3OD) and b) ^{13}C $\{^1\text{H}\}$ -NMR (300 MHz, CD_3OD) spectra of compound G_2 - $[[\text{NCP}h(o\text{-N})\text{Ru}(\eta^6\text{-}p\text{-cymene})\text{Cl}]\text{Cl}]_8$ (**18**).

(a)



(b)

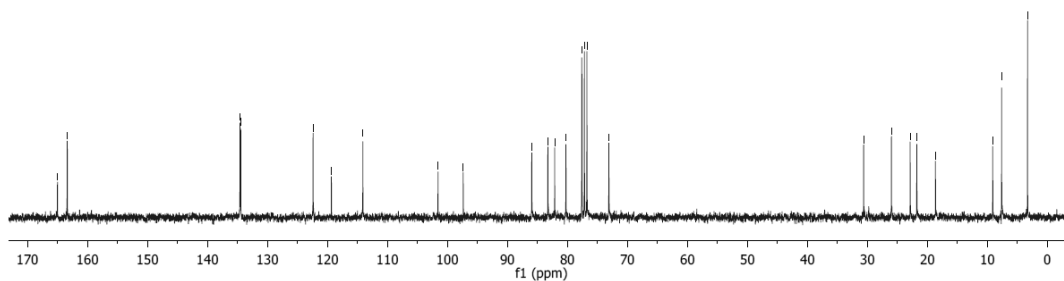
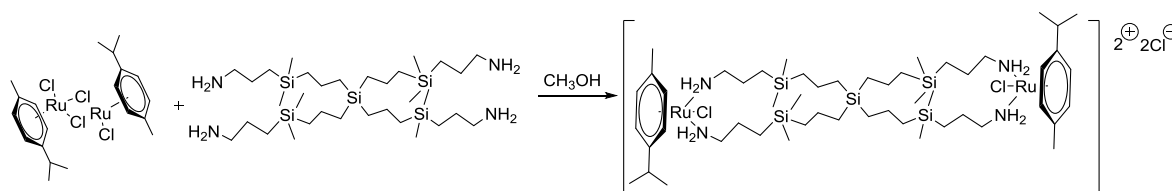


Fig. S17 a) ^1H -NMR (300 MHz, CDCl_3) and b) ^{13}C $\{^1\text{H}\}$ -NMR (300 MHz, CDCl_3) spectra of compound $\text{G}_0\text{-}[\text{NCPPh}(o\text{-O})\text{Ru}(\eta^6\text{-}p\text{-cymene})\text{Cl}]_1$ (**19**).

5. ^1H and ESI-TOF mass spectra of the reaction S1



Scheme S1 1 equivalent of ruthenium with 1 equivalent of the G₇-[NH₂]₄ (**II**).

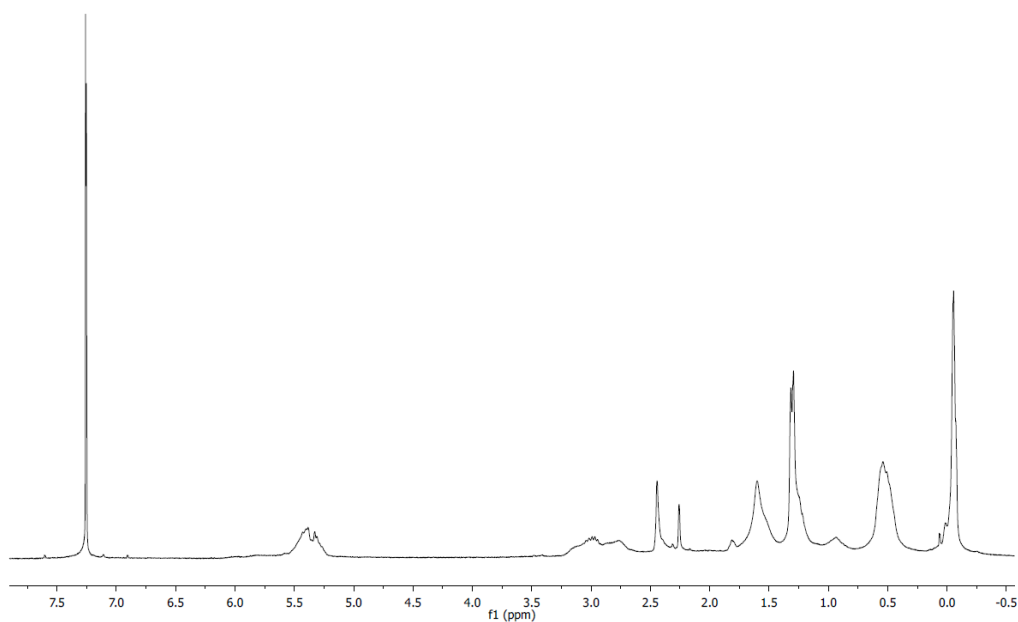


Fig. S18 $^1\text{H-NMR}$ (300 MHz, CDCl₃) spectra of reaction S1.

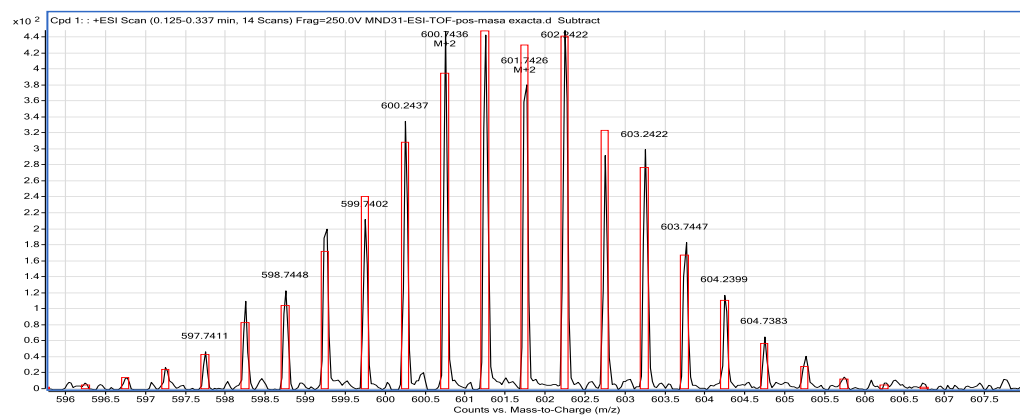
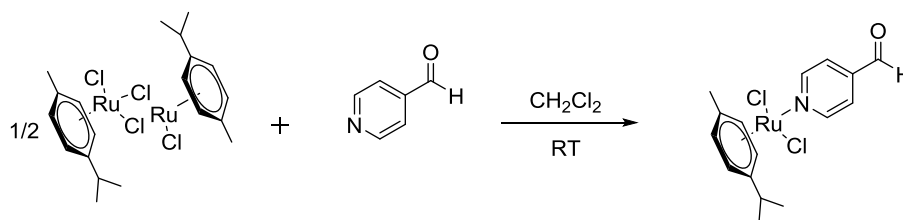


Fig. S19 ESI-TOF mass spectra of reaction S1.

6. ^1H and ^{13}C -NMR spectra of the reaction S2



Scheme S2 $\frac{1}{2}$ equivalent of [Ru] with 1 equivalent of the commercial 4-pyridinecarboxaldehyde.

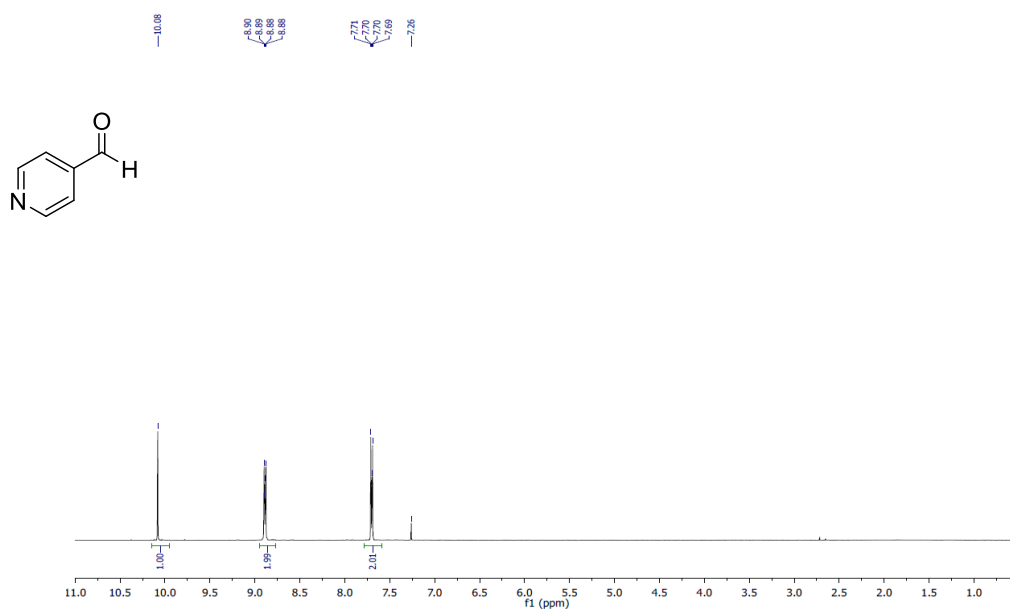


Fig. S20 ^1H -NMR spectra of commercial 4-pyridinecarboxaldehyde.

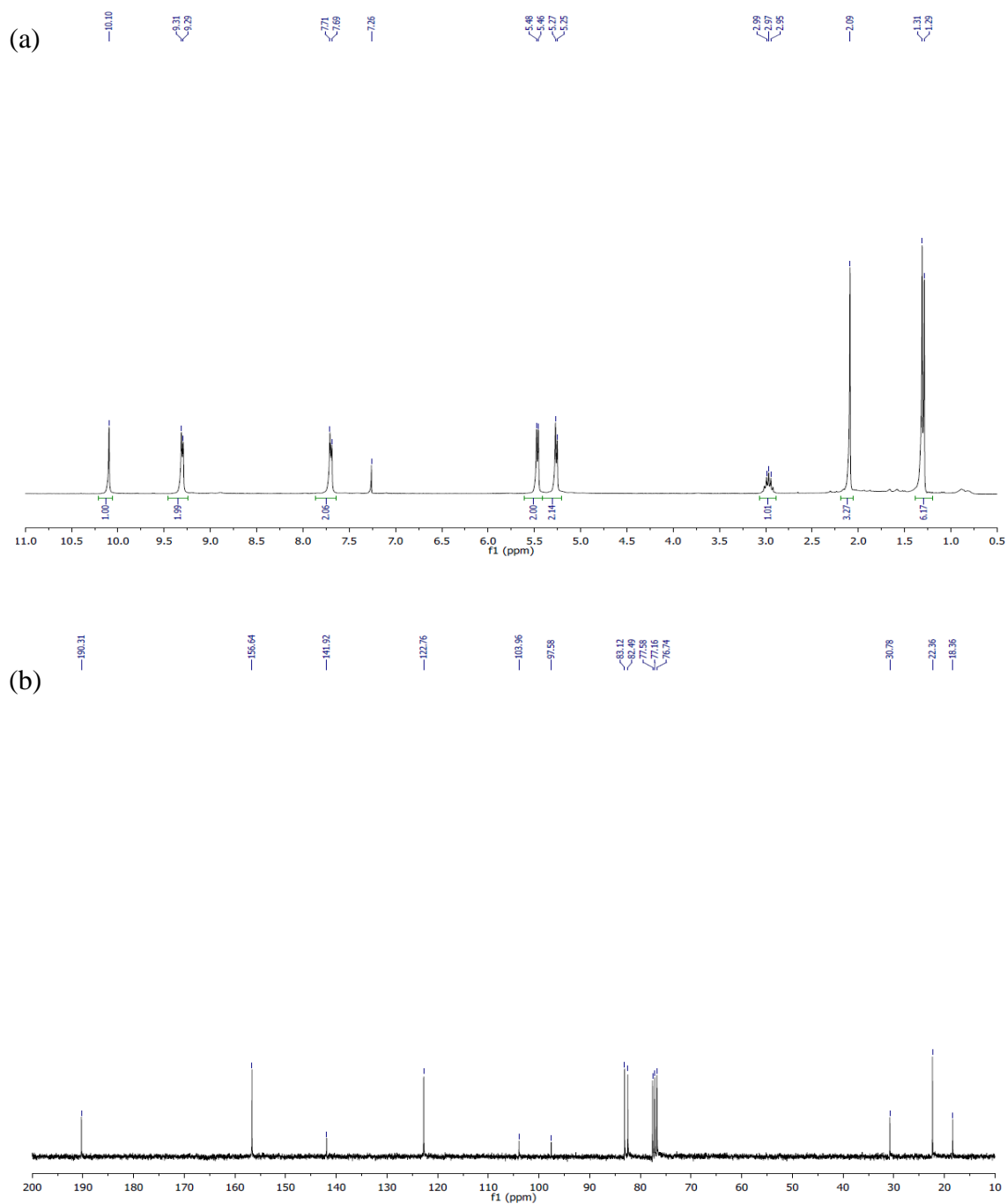
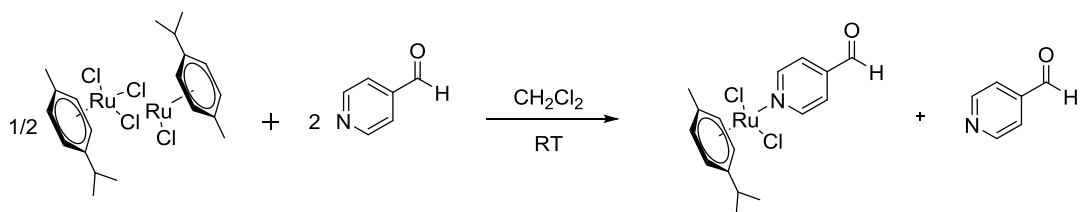


Fig. S21 a) ^1H -NMR (300 MHz, CDCl_3) and b) ^{13}C $\{^1\text{H}\}$ -NMR (300 MHz, CDCl_3) spectra of reaction S2.

7. ^1H and ^{13}C -NMR spectra of the reaction S3



Scheme S3 $\frac{1}{2}$ equivalent of [Ru] with 2 equivalents of the commercial 4-pyridinecarboxaldehyde.

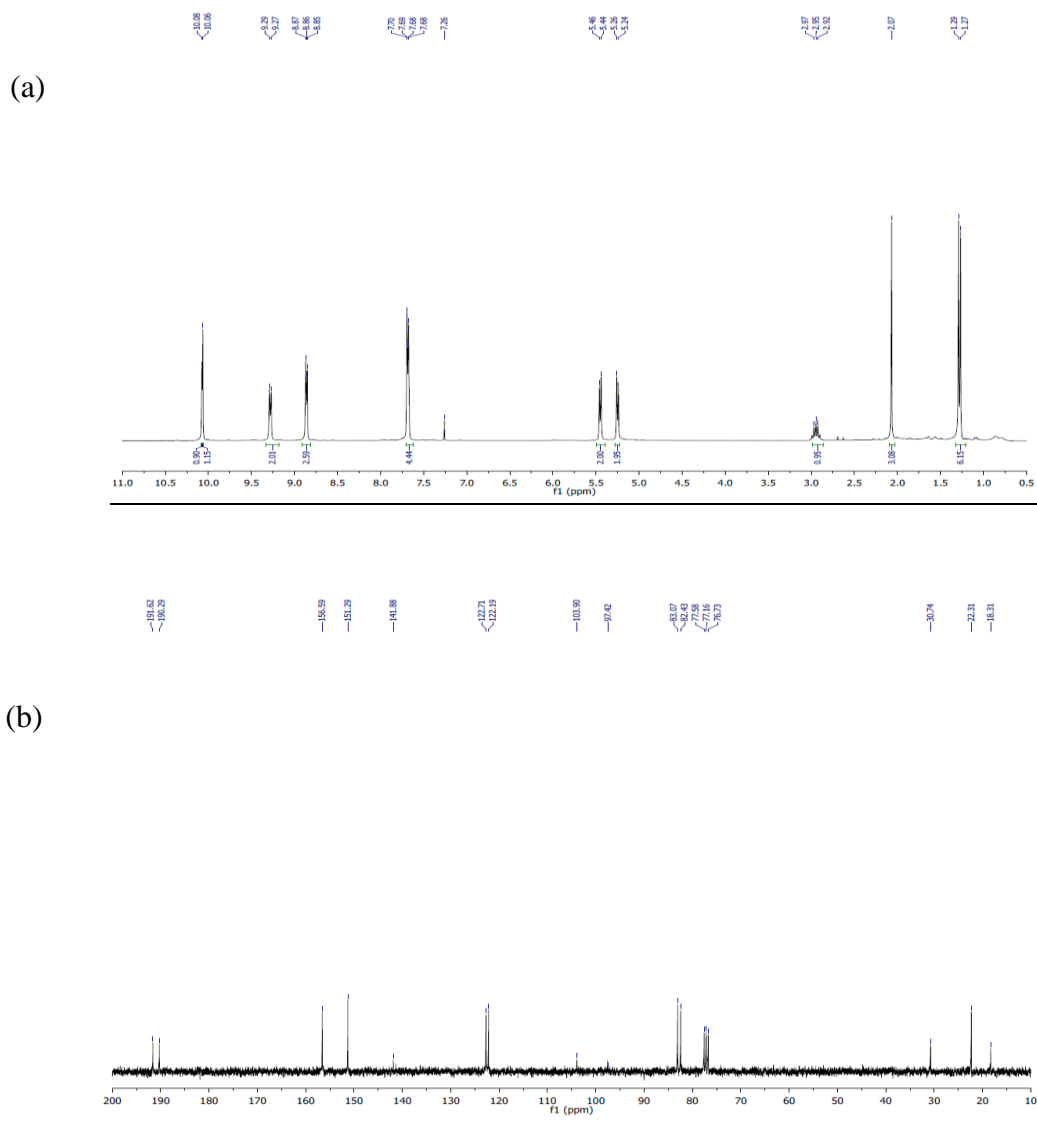


Fig. S22 a) ^1H -NMR (300 MHz, CDCl_3) and b) ^{13}C $\{^1\text{H}\}$ -NMR (300 MHz, CDCl_3) spectra of reaction S3.

8. Stability tests

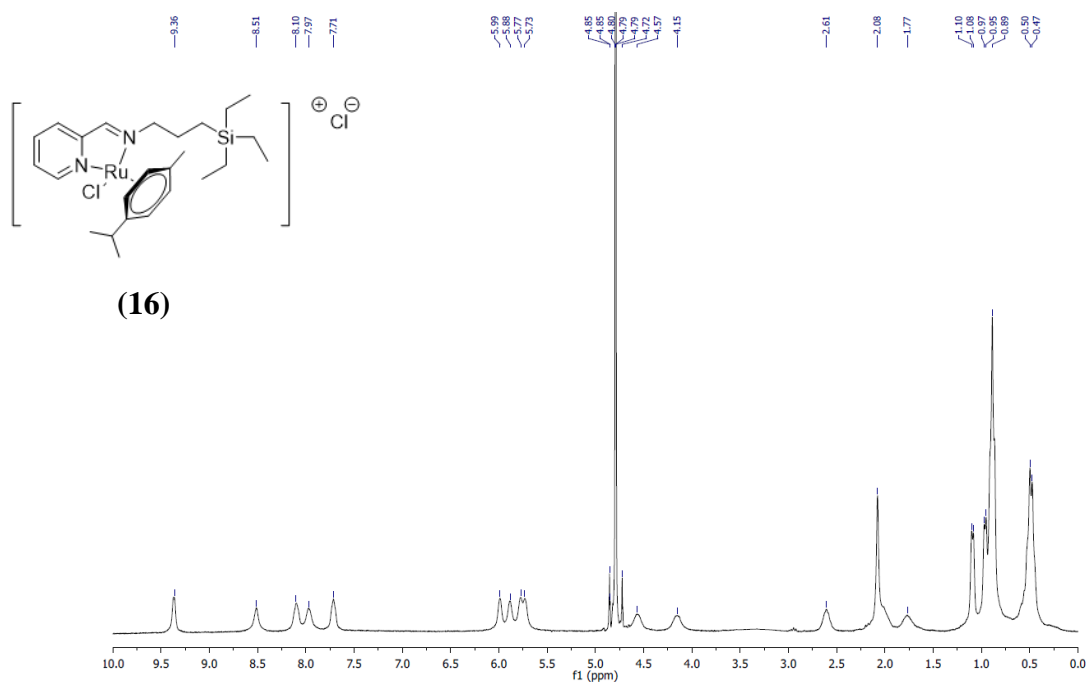


Fig. S23 $^1\text{H-NMR}$ (300 MHz, D_2O) of complex **16**.

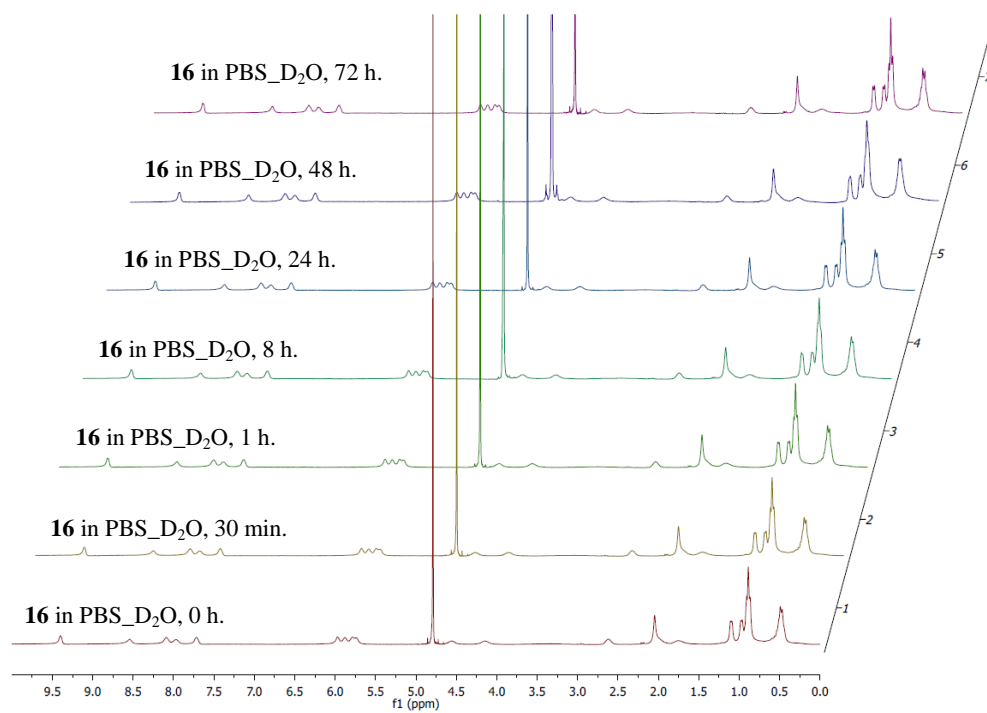


Fig. S24 Time dependent $^1\text{H-NMR}$ (300 MHz, PBS- D_2O) of complex **16** (pH = 7.4).

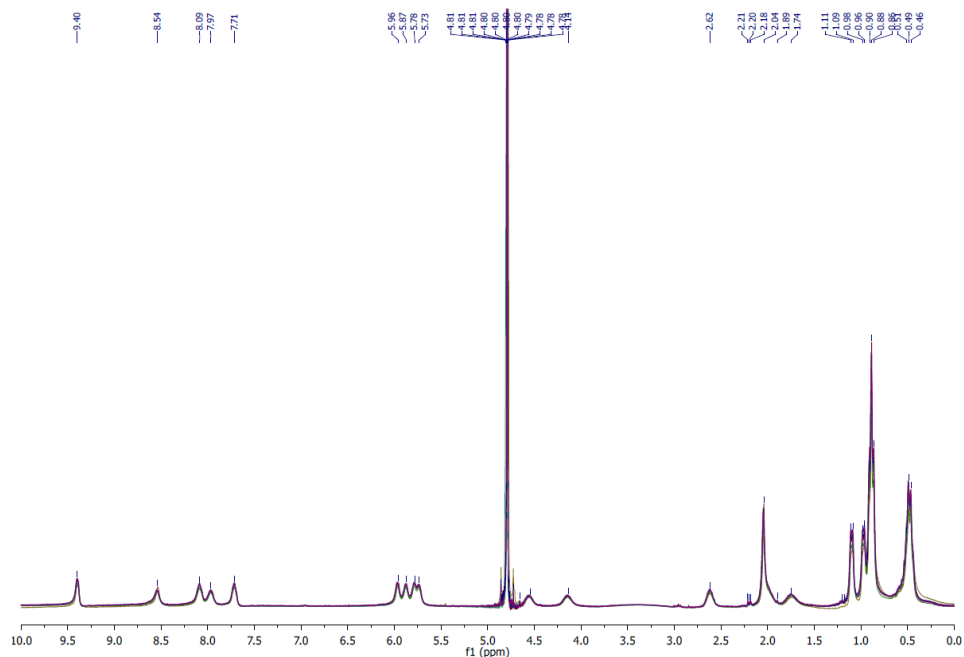


Fig. S25 Time dependent (from 0 to 72h) overlap $^1\text{H-NMR}$ (300 MHz, $\text{PBS-D}_2\text{O}$) of complex **16** (pH = 7.4).

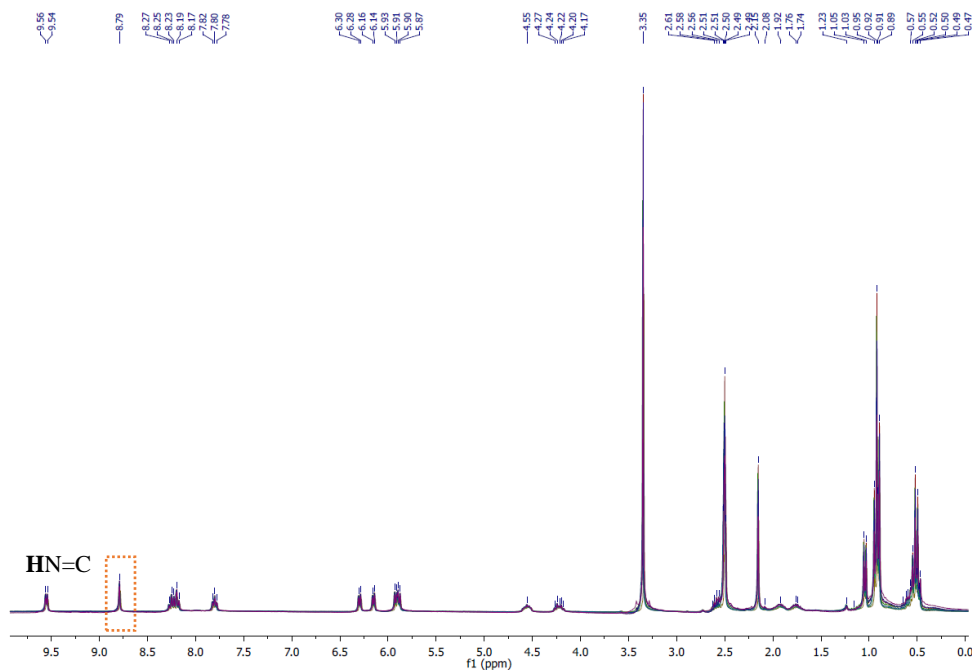


Fig. S26 Time dependent (from 0 to 72h) overlap $^1\text{H-NMR}$ (300 MHz, $\text{DMSO-}d_6$) of complex **16**.

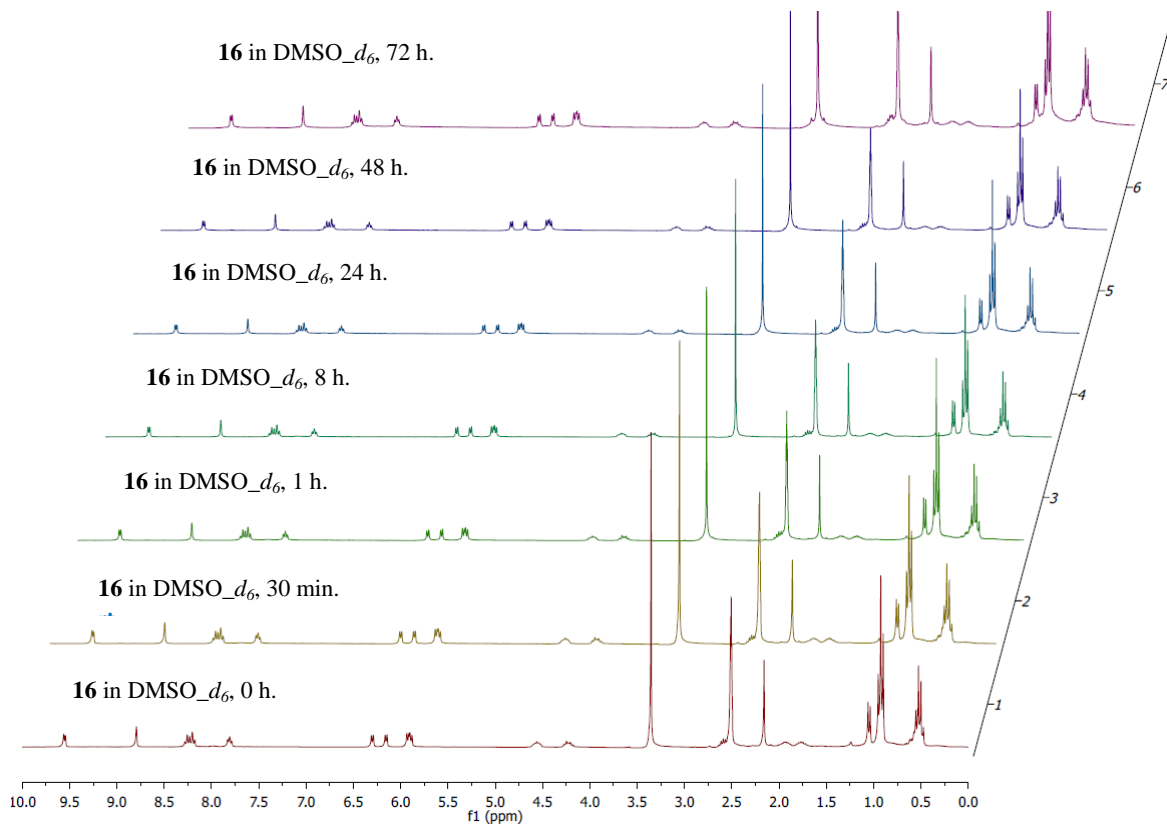


Fig. S27 Time dependent ¹H-NMR (300 MHz, DMSO-*d*₆) of complex **16**.

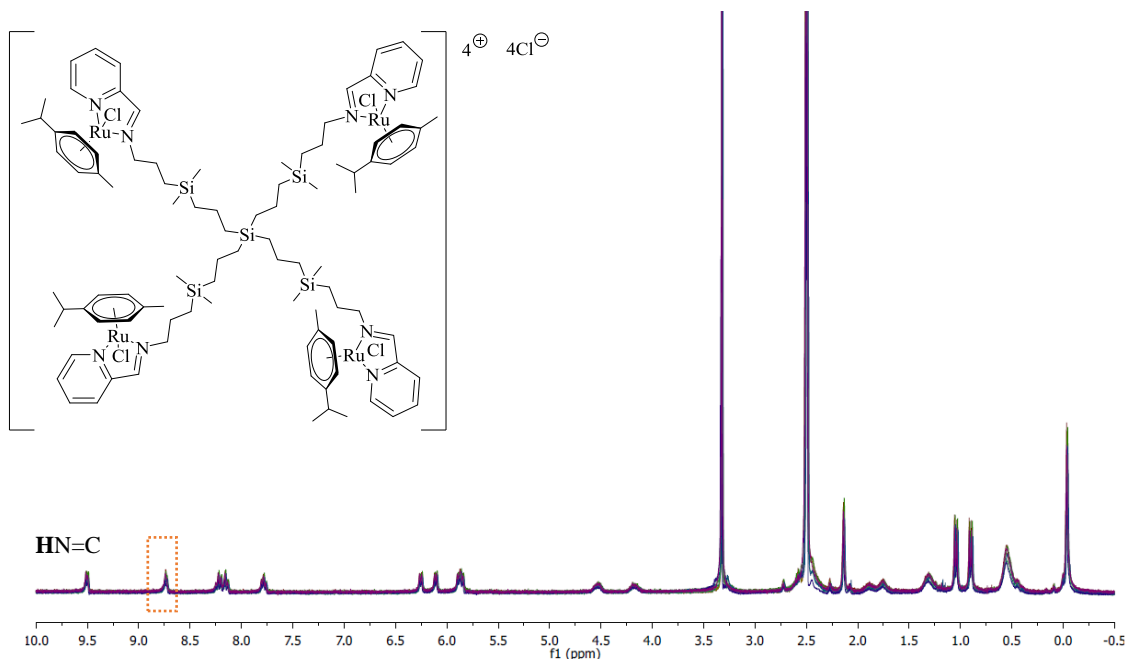


Fig. S28 Time dependent (from 0 to 72h) overlap $^1\text{H-NMR}$ (300 MHz, $\text{DMSO-}d_6$) of complex **17**.

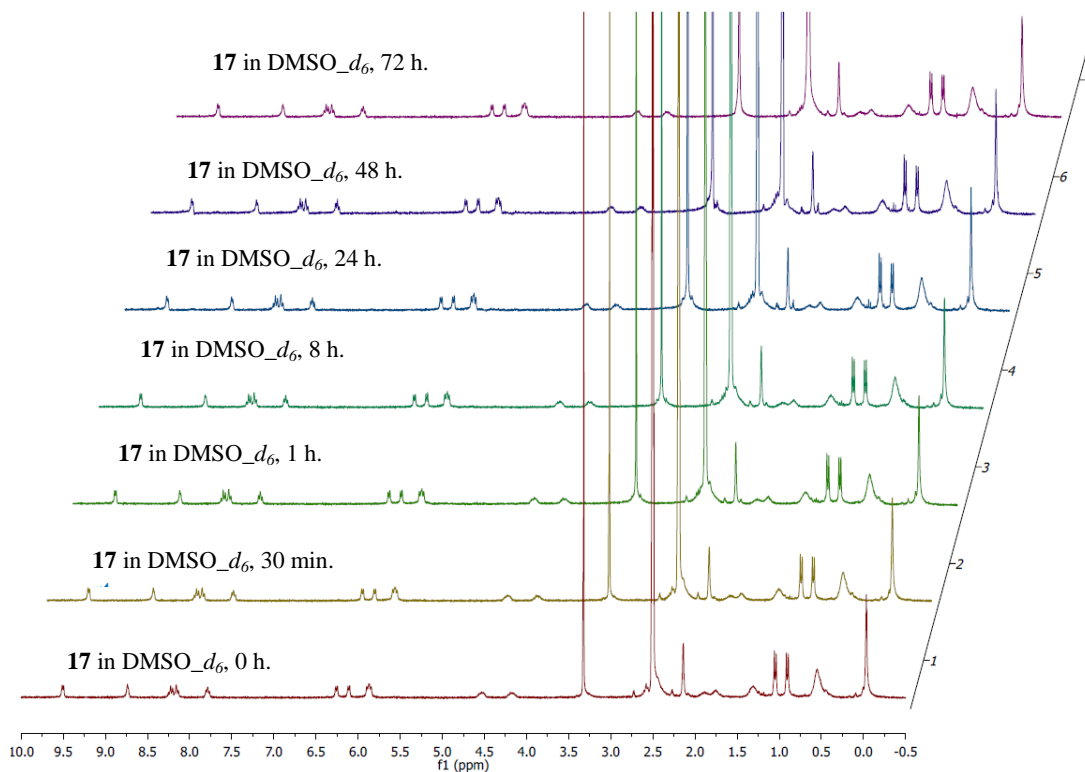


Fig. S29 Time dependent $^1\text{H-NMR}$ (300 MHz, $\text{DMSO-}d_6$) of complex **17**.

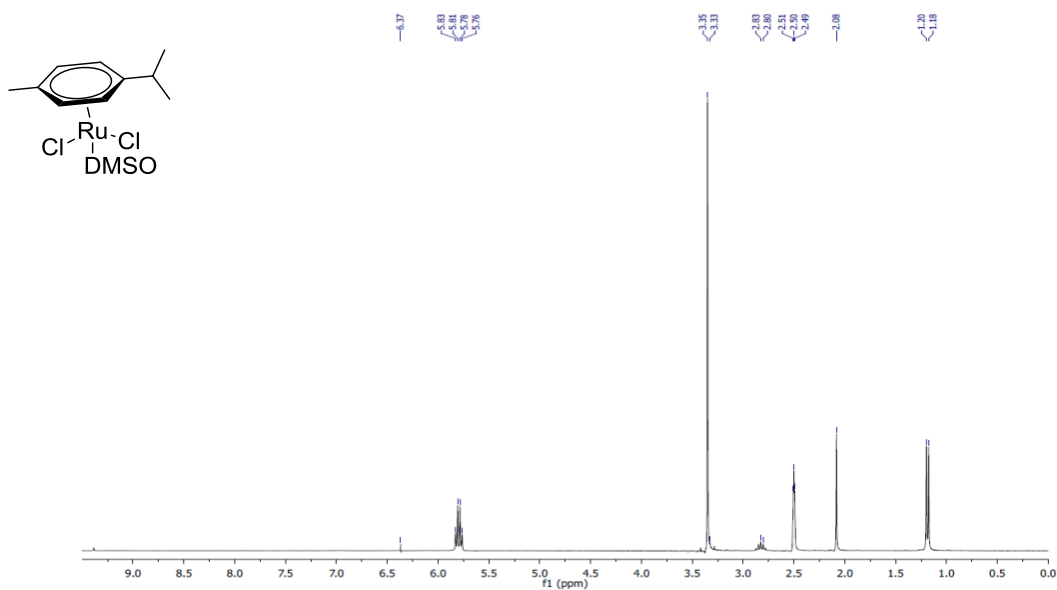


Fig. S30 $^1\text{H-NMR}$ (300 MHz, $\text{DMSO-}d_6$) of complex $[\text{Ru}(\eta^6\text{-}p\text{-cymene})\text{Cl}_2(\text{DMSO})]$.

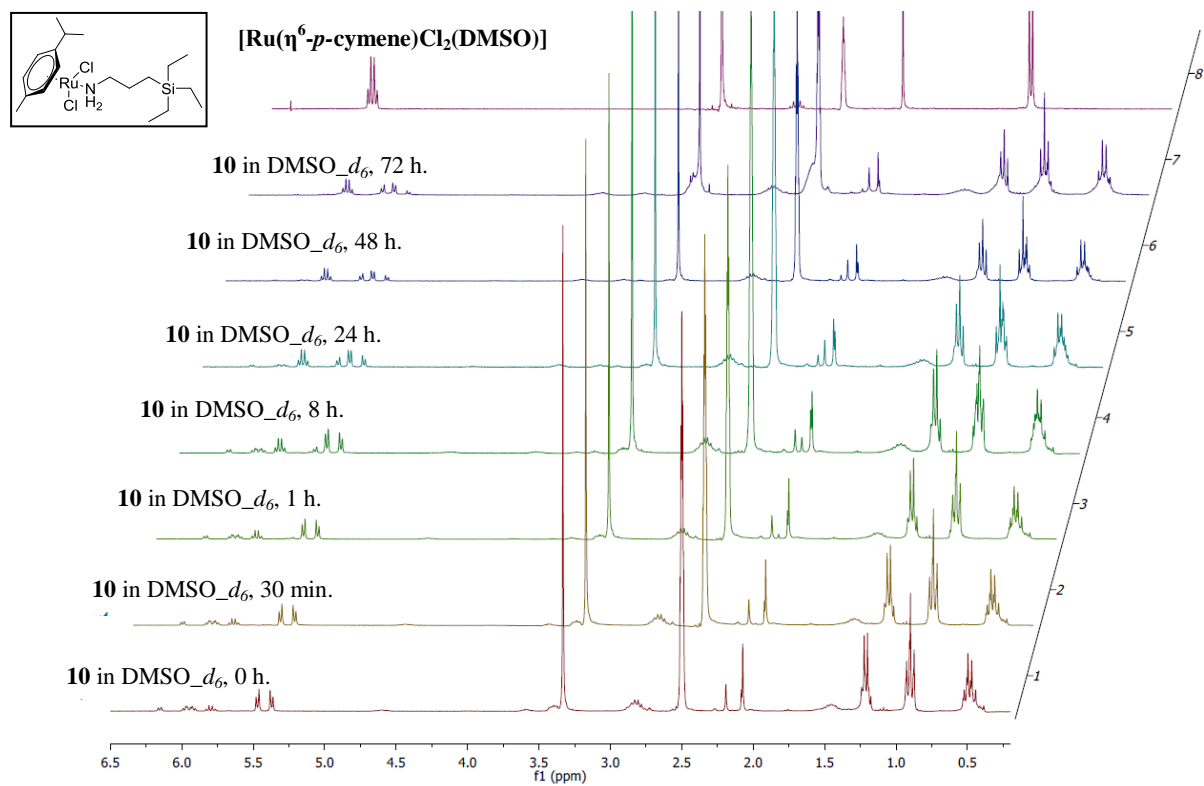


Fig. S31 Time dependent $^1\text{H-NMR}$ (300 MHz, $\text{DMSO-}d_6$) of complex **10**.

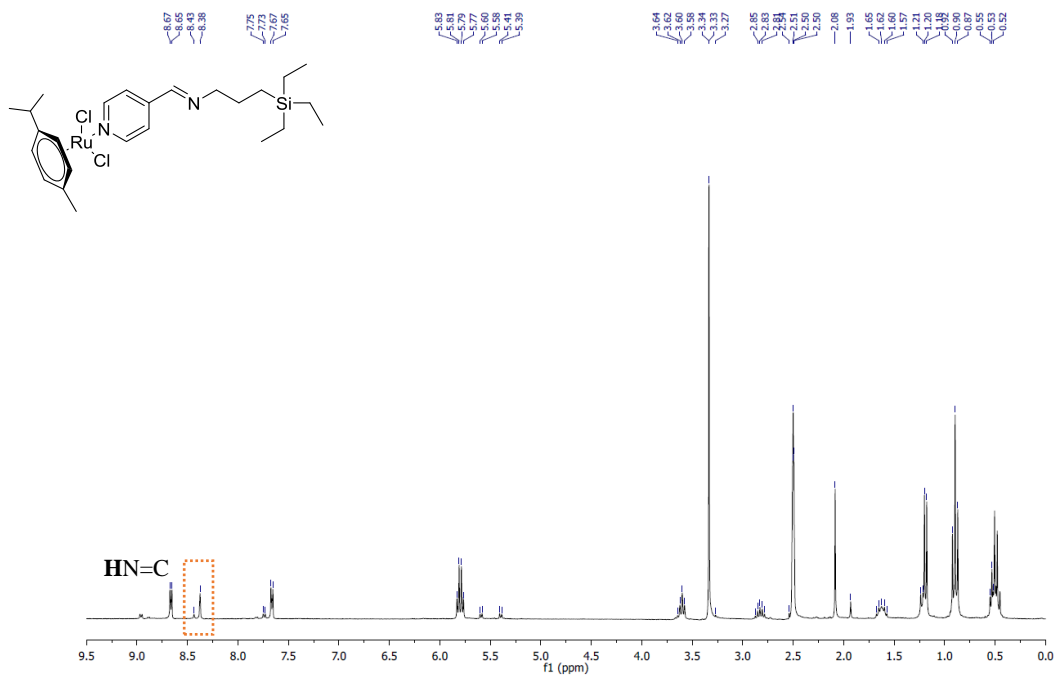
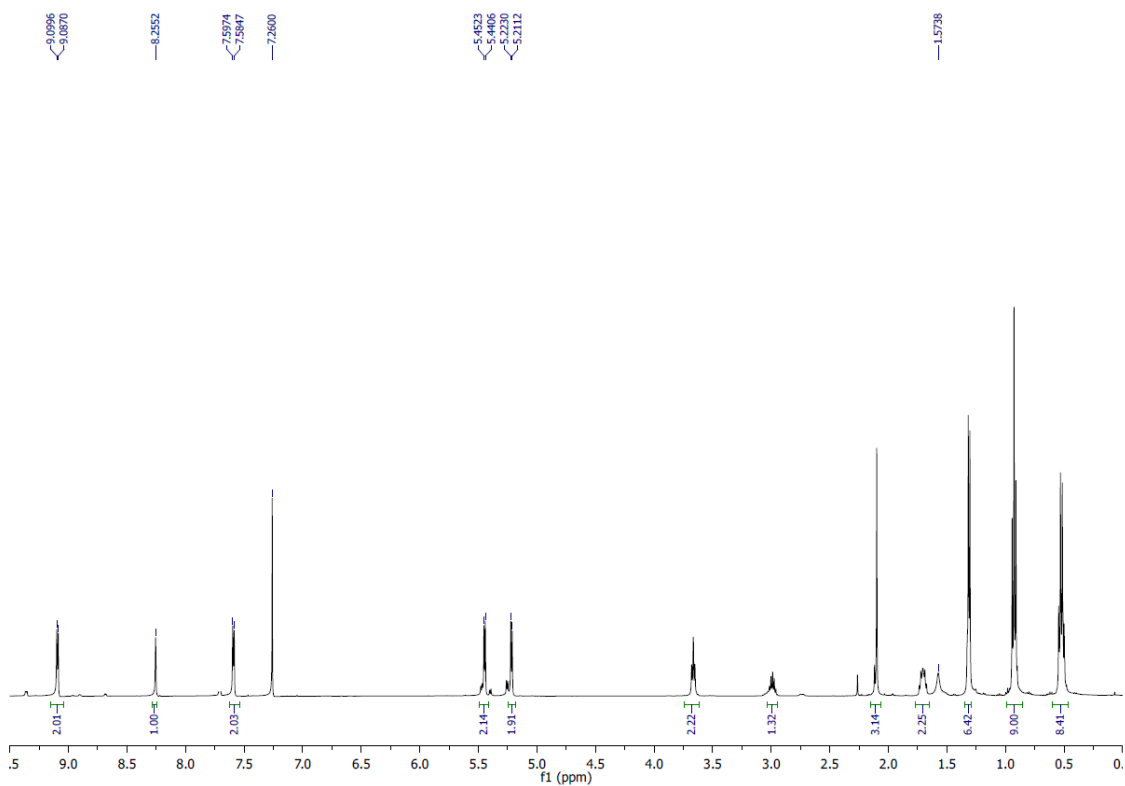


Fig. S32 $^1\text{H-NMR}$ (300 MHz, $\text{DMSO-}d_6$) of complex 13.



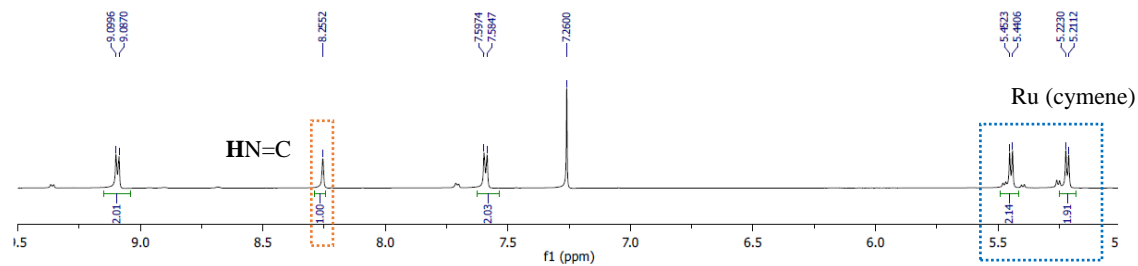


Fig. S33 $^1\text{H-NMR}$ (300 MHz, CDCl_3) of complex **13**.

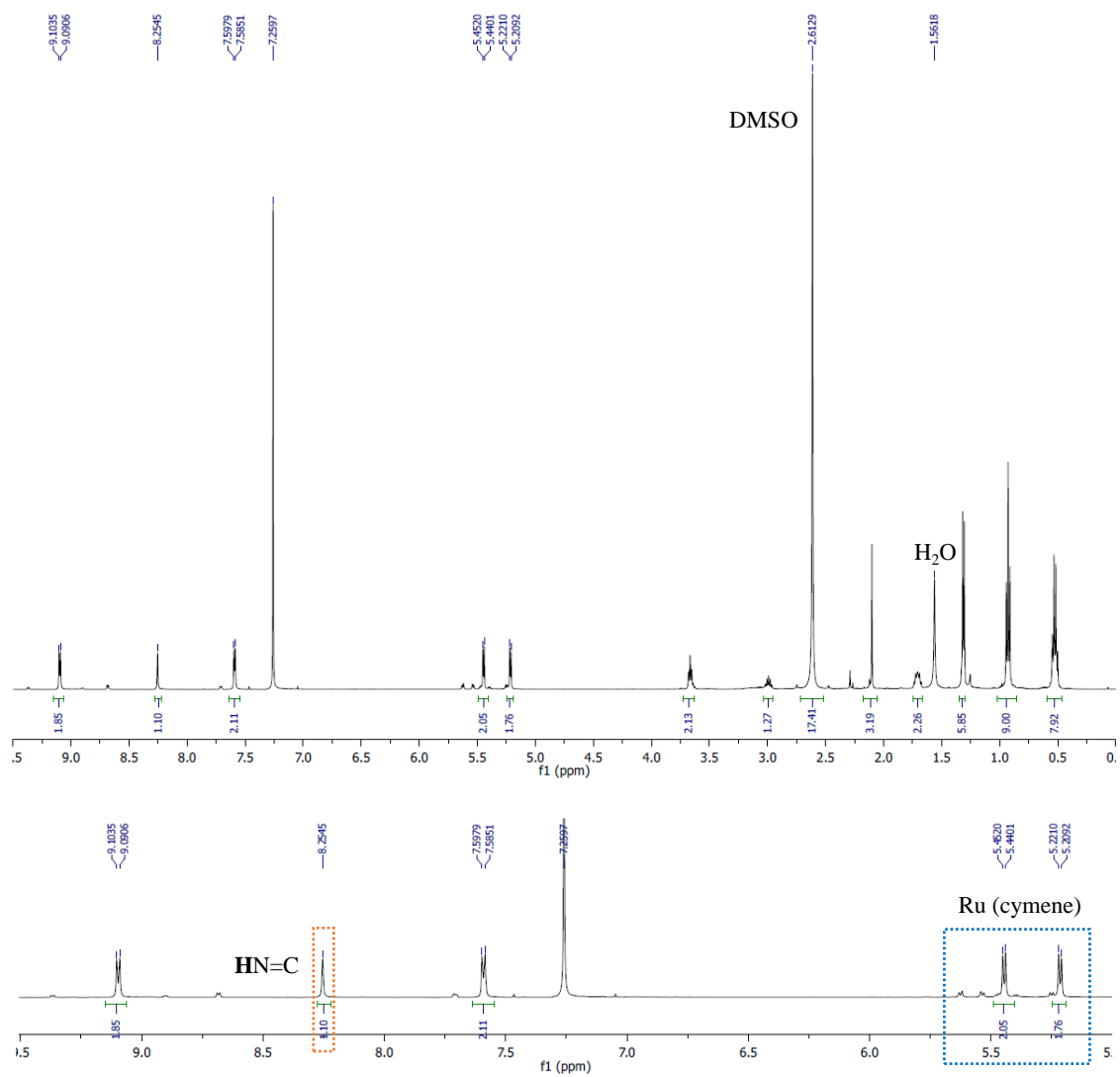


Fig. S34 $^1\text{H-NMR}$ (300 MHz, $\text{CDCl}_3/\text{DMSO}$ (1:4)) of complex **13**.

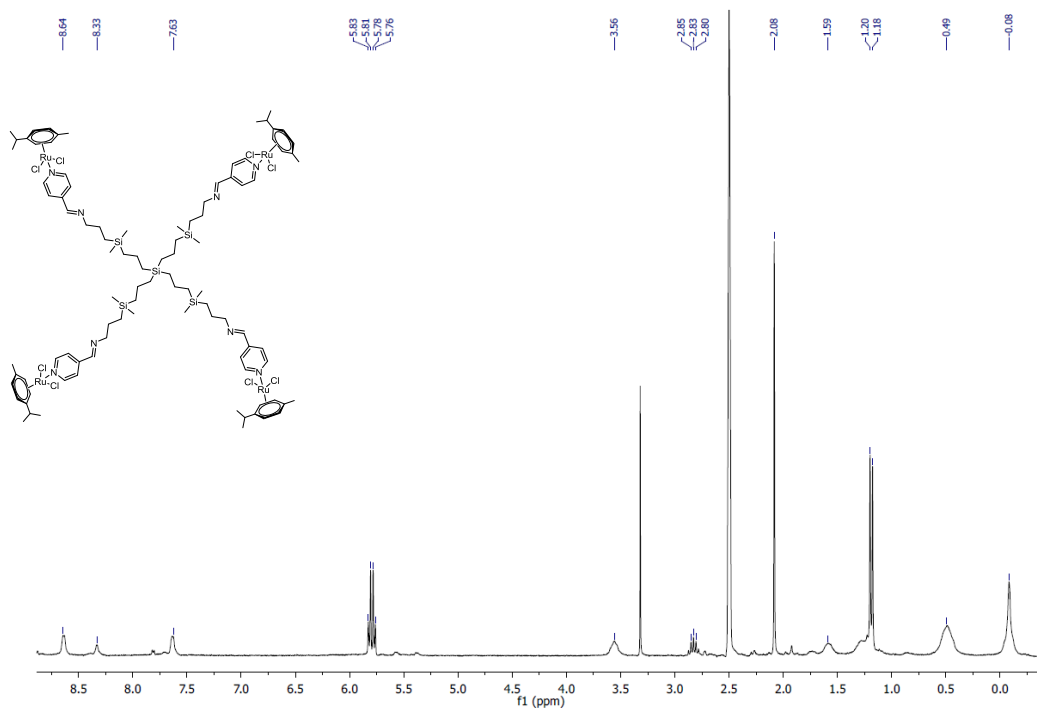


Fig. S35 $^1\text{H-NMR}$ (300 MHz, $\text{DMSO-}d_6$) of complex **14**.

9. Fluorescence titration curve of HSA with compound **10-11, 13-15, 17-18**

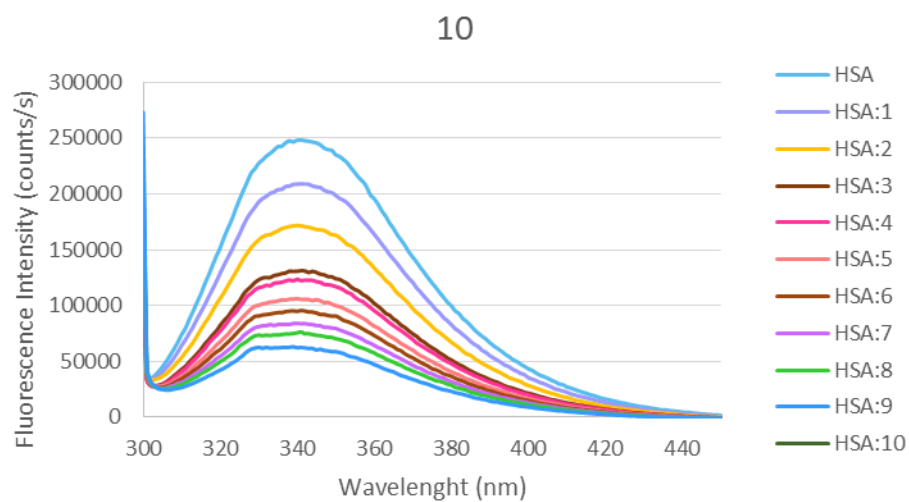


Fig. S36 Fluorescence titration curve of HSA with compound **10**.

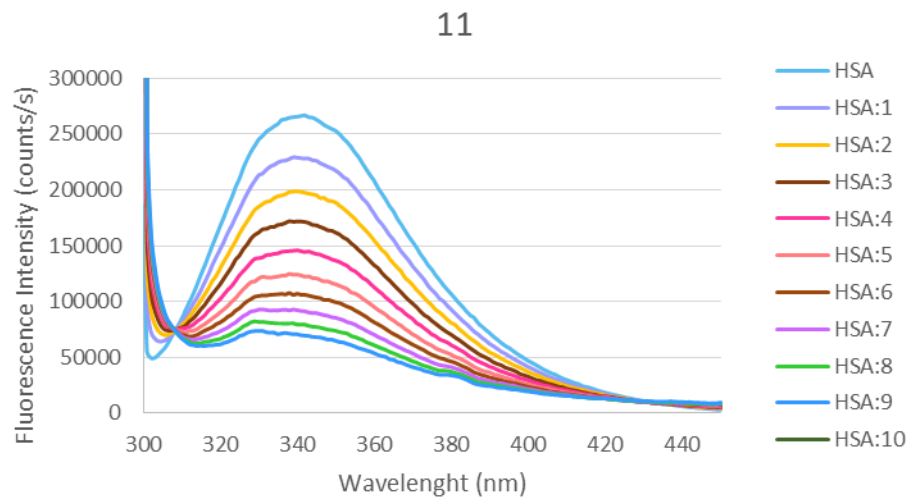


Fig. S37 Fluorescence titration curve of HSA with compound **11**.

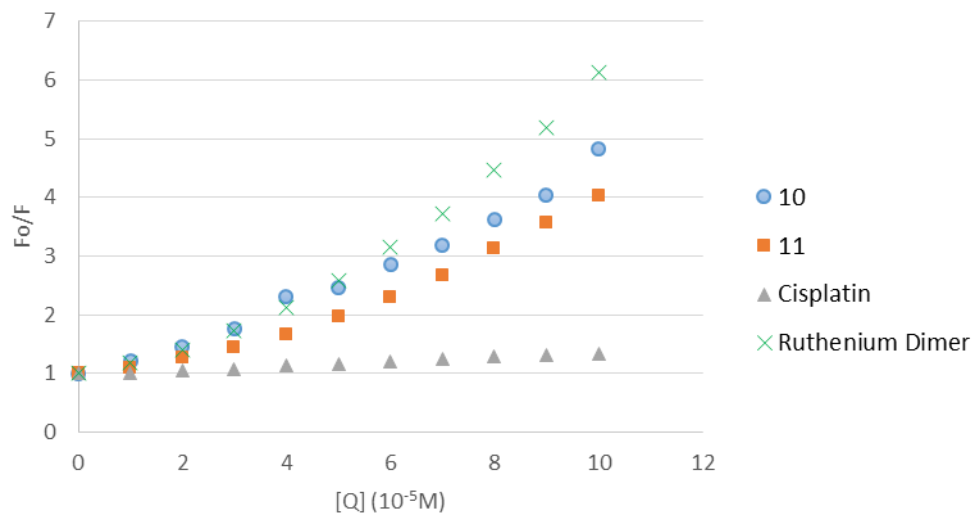


Fig. S38 Stern-Volmer plot for HSA fluorescence quenching observed with compound **10**, **11**, the ruthenium dimer $[Ru(\eta^6-p\text{-cymene})Cl_2]_2$ and cisplatin.

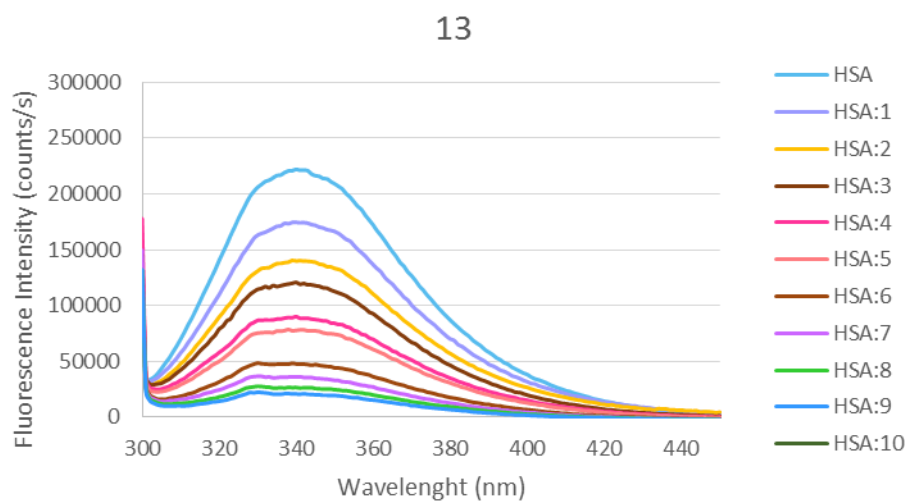


Fig. S39 Fluorescence titration curve of HSA with compound **13**.

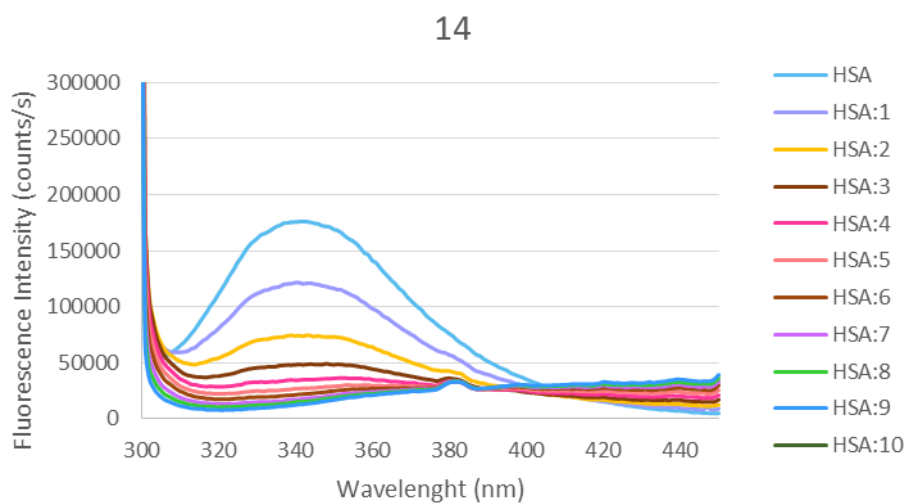


Fig. S40 Fluorescence titration curve of HSA with compound **14**.

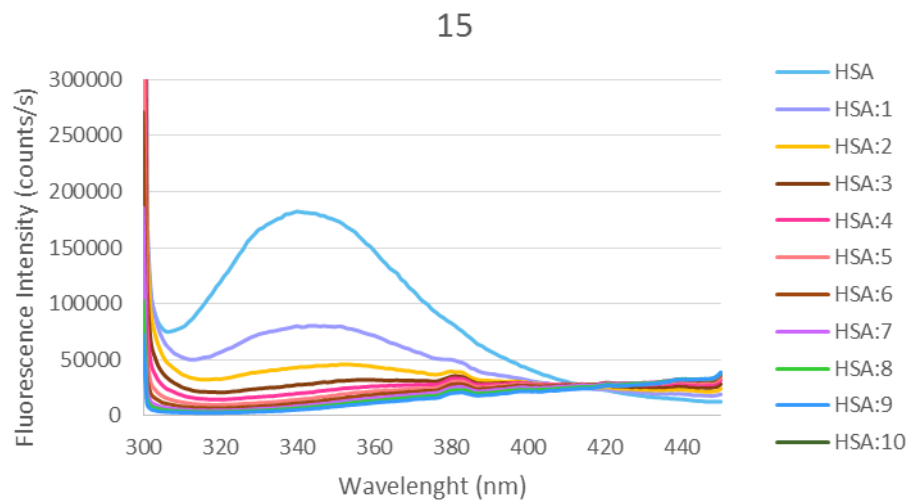


Fig. S41 Fluorescence titration curve of HSA with compound **15**.

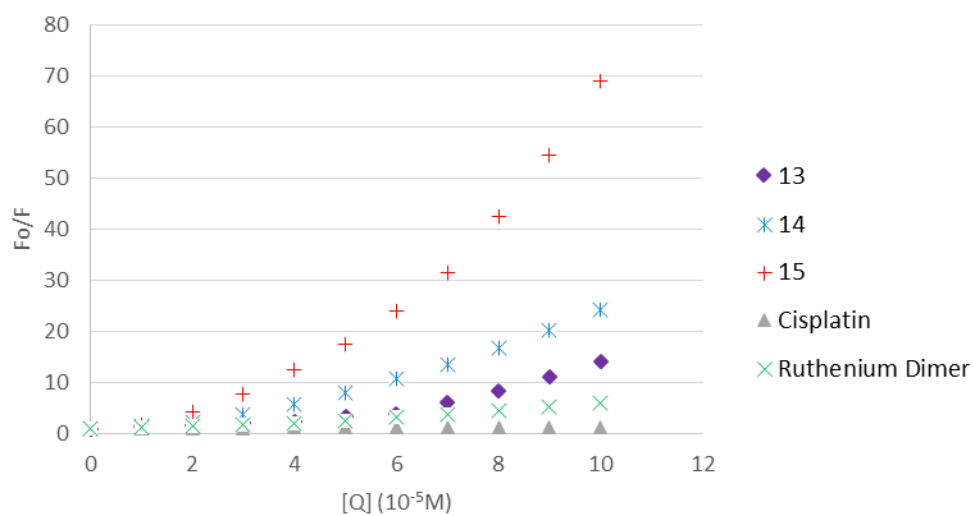


Fig. S42 Stern-Volmer plot for HSA fluorescence quenching observed with compound **13**, **14**, **15**, the ruthenium dimer $[Ru(\eta^6\text{-}p\text{-cymene})Cl_2]_2$ and cisplatin.

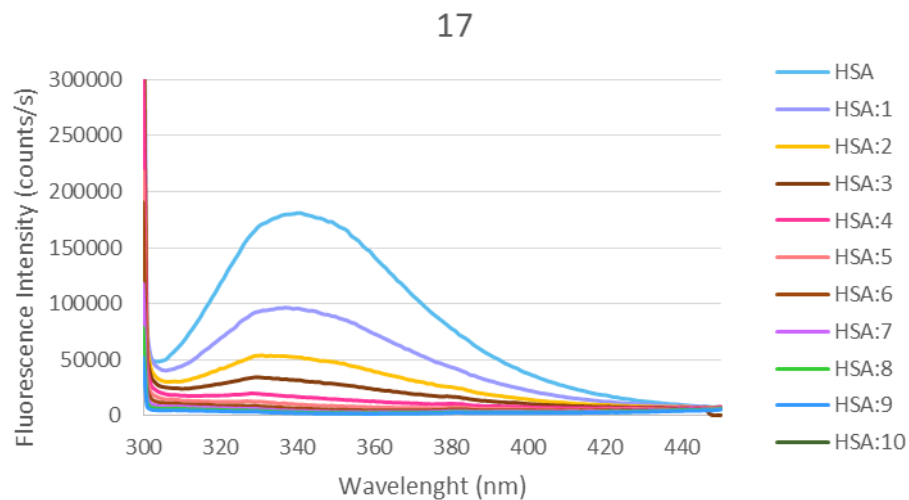


Fig. S43 Fluorescence titration curve of HSA with compound **17**.

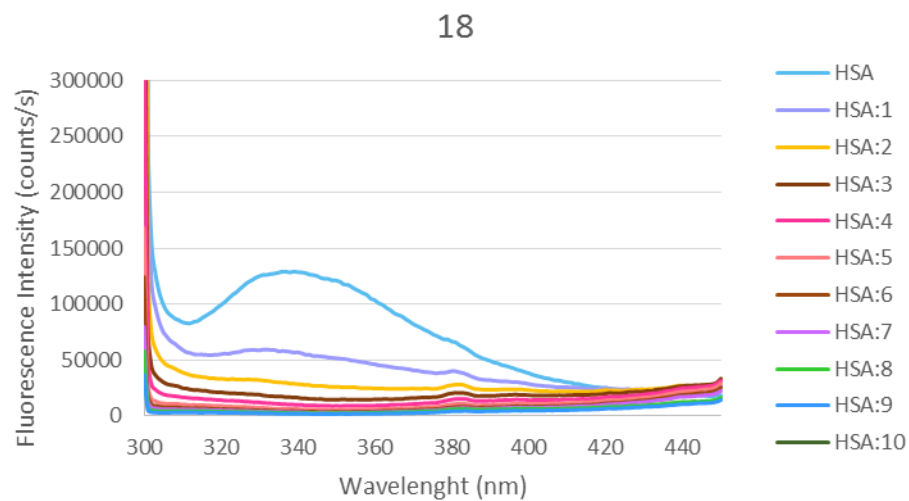


Fig. S44 Fluorescence titration curve of HSA with compound **18**.

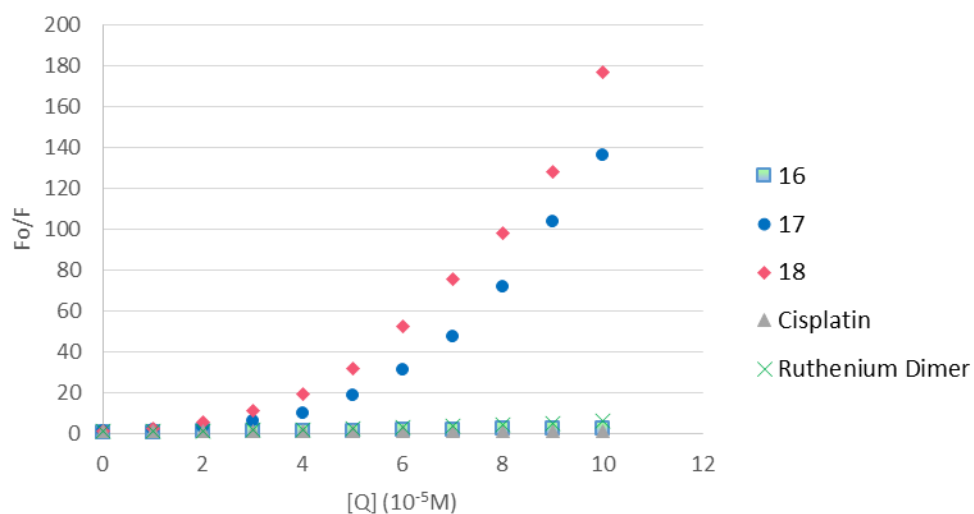


Fig. S45 Stern-Volmer plot for HSA fluorescence quenching observed with compound **16**, **17**, **18**, the ruthenium dimer $[\text{Ru}(\eta^6\text{-}p\text{-cymene})\text{Cl}_2]_2$ and cisplatin.

10. Crystal and structure refinement data for compound **10**

Table S1 Crystal and structure refinement data for compound **10**.

Empirical formula	$\text{C}_{19}\text{H}_{37}\text{Cl}_2\text{NRuSi}$
Formula weight	479.57
Crystal system, space group	Triclinic, P -1
Unit cell dimensions	
A	7.2564(5) Å
B	11.7148(10) Å
C	13.8168(14) Å
α	78.098(8)°

β	82.292(5)°
γ	85.667(6)°
Volume, Å^3	1137.50(17) - Å^3
Z, Cal.density Mg/m^3	2,1.400
Absorption coefficient mm^{-1}	0.979
F(000)	500
Crystal size, mm	0.30 x 0.26 x 0.2
θ range for data collection	3.04° to 27.50°
Limiting indices	-9 \leq h \leq 9, -15 \leq k \leq 15, -17 \leq l \leq 17
Reflections collected /unique	9855 / 5217 [R(int) = 0.0858]
Completeness to θ	$\theta = 27.50$; 99.8 %
Absorption correction	Multi-scan
Max. and min. transmission	0.864 and 0.649
Refinement method	Full-matrix least-squares on F ²
Data / restraints / parameters	5217 / 0 / 217
Goodness-of-fit on F ²	0.755
Final R indices [I $>$ 2 σ (I)]	R1 = 0.0487, wR2 = 0.1049
R indices (all data)	R1 = 0.980, wR2 = 0.1253
Largest diff. peak and hole $\text{e}^{-3} \text{Å}$	0.712 and -0.637

Table S2 Selected bond lengths (Å) and angles (°) for compound **10**.

Selected bond lengths (Å) for compound 10.			
Ru(1)-Cl(1)	2.4246 (12)	Ru (1)-C(4)	2.203 (5)
Ru(1)-Cl(2)	2.4126 (12)	Ru (1)-C(1)	2.208 (5)
Ru(1)-N(1)	2.135 (4)	N(1)-C(11)	1.475 (6)
Ru(1)-Cent	1.668	Si(1)-C(18)	1.861 (5)
Ru(1)-C(5)	2.163 (5)	Si(1)-C(16)	1.864 (6)
Ru(1)-C(3)	2.165 (4)	Si(1)-C(14)	1.877 (6)
Ru(1)-C(2)	2.184 (4)	Si(1)-C(13)	1.878 (5)
Ru(1)-C(6)	2.192 (5)		
Selected bond angles (°) for compound 10.			
N(1)-Ru(1)-Cl(2)	80.51 (11)	C(18)-Si(1)-C(16)	108.7 (3)
N(1)-Ru(1)-Cl(1)	80.89 (11)	C(18)-Si(1)-C(14)	109.0 (3)
Cl(2)-Ru(1)-Cl(1)	87.79 (5)	C(16)-Si(1)-C(14)	110.2 (3)
Cent*-Ru(1)-Cl(1)	128.24	C(18)-Si(1)-C(13)	109.4 (2)
Cent*-Ru(1)-Cl(1)	128.63	C(16)-Si(1)-C(13)	107.6 (2)
Cent*-Ru(1)-Cl(1)	133.35	C(14)-Si(1)-C(13)	111.9 (3)
C(11)-N(1)-Ru(1)	120.2 (3)		
*Cent is the centroid of C1 C2 C3 C4 C5 C6.			